Investigation of PI3K/AKT signaling pathway in canine soft tissue sarcoma

犬の軟部組織肉腫における **PI3K/AKT** シグナル伝達経路の検討

Joint Graduate School of Veterinary Medicine

Yamaguchi University

Alfarisa Nururrozi

March 2025

SUMMARY

Soft tissue sarcoma (STS) is one of the most common cancers in dogs. Canine STS encompasses a heterogeneous group of mesenchymal neoplasia, accounting for approximately 8–15% of all canine cancers. These tumors can originate from various soft tissues, resulting in diverse histological subtypes that exhibit distinct biological behaviors and therapeutic responses. The primary challenge in canine STS is the lack of reliable prognostic markers and an incomplete understanding of its pathogenesis. This research investigates the phosphatidylinositol-3 kinase (PI3K) and protein kinase B (AKT) signaling pathways, as their analysis may provide insights into disease activity and potential prognostic markers. PI3K/AKT is one of the signaling pathways contributing to cell proliferation and is a crucial regulator of various critical cellular processes such as growth, survival, and metabolism. Dysregulation of the PI3K/AKT pathway due to genetic mutations or alterations in its components has contributed to tumorigenesis. Our previous investigation identified the PI3K/AKT pathway activation in STS cell lines and clinical samples. We confirmed that phosphorylation of AKT occurred in conjunction with S6 phosphorylation in three canine STS cell lines (MUMA-G, A72, and STS-YU1) based on western blotting, as compared with a mouse fibroblast cell line (NIH3T3).

The first chapter investigated the relationship between PI3K/AKT activation and tumor-infiltrating lymphocytes (TILs), as the dysregulation of this pathway may influence TILs density within the tumor microenvironment (TME). 59 STS samples were labeled via immunohistochemistry to calculate the density of TILs, including CD3+ T cells, CD8+ T cells, CD20+ B cells, and FOXP3+ regulatory T cells. Most canine STS samples (81.3%) contained intra-tumoral TILs, with CD3+ T cells and CD8+ T cells being the most abundant, while CD20+ B cells and FOXP3+ T-regulatory cells were comparatively limited. This TILs profile indicates that the immune response in dogs remains favorable against STS, as CD3+ and CD8+ T cells subsets are critical for cytotoxic responses against cancer. TILs density, however, was not associated with clinicopathological parameters and tumor grade.

Furthermore, a positive correlation between TILs density and the Ki-67 index, a tumor proliferation marker. Samples with a high Ki-67 index had a significantly higher abundance of CD3+ T cells, CD8+ T cells, and CD20+ B cells (p=0.0392, 0.0254, 0.0380, respectively). This finding provides initial insights into the role of PI3K/AKT pathway activation in canine STS. The abundance of CD8+ T cells was positively correlated with the activation of PI3K/AKT, indicating that samples with high levels of phospho-AKT and

phospho-S6 tend to have higher CD8+ T cell densities (p=0.0032 and 0.0218, respectively). These findings suggest that the PI3K/AKT signaling pathway might play a role in modulating the immune landscape. A plausible mechanism is that elevated PI3K/AKT pathway activity in cancer cells indirectly enhances tumor-antigen presentation or promotes the secretion of chemokine molecules to attract immune cells to the tumor site.

The second chapter investigated the underlying mechanism as a primary contributor to PI3K/AKT dysregulation, possibly contributing to tumorigenesis in canine STS. This chapter investigated PTEN loss, *PIK3CA* mutation, and EGFR over-expression as potential PI3K/AKT pathway activation drivers. The investigation suggests that EGFR over-expression, rather than PTEN loss and *PIK3CA* mutations, is likely a primary driver of pathway dysregulation. While PTEN loss is one of the common mechanisms for PI3K/AKT dysregulation, there is no evidence of PTEN loss in canine STS samples. PTEN was expressed in all analyzed samples. Weak PTEN expression was observed in 33.3% of samples, while 66.7% showed normal expression.

Although mutations in *PIK3CA* and *EGFR* genes were detected, their low prevalence suggests they are not the primary cause of pathway dysregulation. DNA sequencing of the *PIK3CA* gene revealed a missense point mutation in exon 10 (c.554 A>C, H554P) in only one case, but no hotspot mutations were identified. Similarly, one missense point mutation in exon 21 of *EGFR* (c.868 G>A) was identified in one sample. High EGFR expression was significantly correlated with elevated phospho-AKT levels (p<0.0001) based on a linear regression test. EGFR was expressed in 83.3% of STS samples; in most cases (90% of EGFR-positive samples), it also showed positive immunolabeling for phospho-AKT. This result indicates that EGFR over-expression is a potential major contributor to the PI3K/AKT pathway dysregulation. When EGFR is over-expressed, it facilitates consecutive activation of the downstream PI3K/AKT signaling pathway, results in cellular changes, and disrupts normal cell regulation.

In conclusion, this study identifies EGFR overexpression as a significant feature and potential contributor to the activation of the PI3K/AKT pathway in canine STS. This finding highlights promising opportunities for the development of targeted therapies in the future. Targeting this receptor using EGFR inhibitors has been explored in human cancer therapy, and similar strategies could be repurposed for dogs. These findings underscore the need for additional research to better understand the molecular mechanisms in canine STS and validate potential therapeutic targets.

TABLE OF CONTENT

LIST OF TABLES

LIST OF FIGURES

ABBREVIATIONS

AKT	Protein kinase B
CCL2	C-C motif chemokine ligand 2
CCL5	C-C motif chemokine ligand 5
CD3	Cluster of differentiation, refers to T cells lymphocytes
CD4	Cluster of differentiation, refers to helper T lymphocytes
CD8	Cluster of differentiation, refers to cytotoxic T lymphocytes
CD20	Cluster of differentiation, refers to B cells lymphocytes
CMT	Canine mammary tumor
CTL	Cytotoxic T lymphocytes
CXCL10	C-X-C motif chemokine ligand 10
CXCL9	C-X-C motif chemokine ligand 9
CXCR3	C-X-C chemokine receptor 3
DNA	Deoxyribonucleic acid
EGF	Epidermal growth factor
EGFR	Epidermal growth factor receptor
EMT	Epithelial-mesenchymal transition
ErbB-1	Refers to a family of epidermal growth factor receptor
ERK	Extracellular signal-regulated kinase
FFPE	Formalin-fixed paraffin-embedded
FOXP3	Forkhead box P3
HE	Hematoxylin-eosin
HER-1	Human epidermal growth factor receptor 1
HPFs	High-power fields
HSA	Hemangiosarcoma
ICAM-1	Intercellular adhesion molecule 1
IgG	Immunoglobulin G
IHC	Immunohistochemistry
JAK	Janus kinase
Ki-67	A nuclear protein that is used as a proliferation marker
LMS	Leiomyosarcoma
LPS	Liposarcoma
mAb	Monoclonal antibody

MNST	Malignant nerve sheath tumor
mTOR	Mechanistic target of rapamycin
MUMA-G	A canine fibrosarcoma cell line
MXS	Myxosarcoma
NIH3T3	A mouse fibroblast cell line
OMM	Oral malignant melanoma
OS	Osteosarcoma
PCR	Polymerase chain reaction
PDK-1	3-phosphoinositide-dependent protein kinase 1
Phospho-AKT	Phosphorylated AKT
Phospho-S6	Phosphorylated S6
PI3K	Phosphatidylinositol-3 kinase
PIK3CA	Phosphoinositide-3-kinase catalytic subunit alpha
PIP2	Phosphatidylinositol (4,5)-bisphosphate
PIP3	Phosphatidylinositol (3,4,5)-trisphosphate
PKB	Protein kinase B
PTEN	Phosphatase and tensin homolog
PWT	Perivascular wall tumor
RAS	Rat sarcoma
RAF	Rapidly accelerated fibrosarcoma
RTK	Receptor tyrosine kinase
S6	Ribosomal protein S6
S6K1	Ribosomal protein S6 kinase
STAT	Signal transducer and activator of transcription
STS-YU1	A canine myxosarcoma cell line
TGF-α	Transforming growth factor-alpha
TILs	Tumor-infiltrating lymphocytes
TME	Tumor microenvironment
TP53	Tumor protein 53
Treg	T regulatory cell
UPS	Undifferentiated pleomorphic sarcoma
VCAM-1	Vascular cell adhesion molecule 1
YUAMEC	Yamaguchi University Animal Medical Center

GENERAL INTRODUCTION

GENERAL INTRODUCTION

Soft tissue sarcoma

Cancer has emerged as a significant concern in veterinary medicine. Cancer incidence in dogs was reported to exceed 1,000 cases per 100,000 dogs per year (Baioni *et al.*, 2017). While precise global epidemiological data remain elusive in veterinary medicine, it is estimated that cancer affects approximately one in three dogs and one in five cats (Argyle and Khanna, 2020). Cancer has been identified as the leading cause of mortality in dogs, accounting for 27% of all deaths (Adams *et al.*, 2010). Another study reported that 30-50% of deaths in elderly dogs are attributable to cancer (Sarver *et al.*, 2022). Topographically, cancers in dogs are predominantly observed in the skin (34.64%), followed by soft tissues (20.17%) and mammary glands (14.50%) (Dhein *et al.*, 2024).

Soft tissue sarcoma (STS) is one of the most common cancers in dogs (Bray, 2016). Canine STS encompasses a heterogeneous group of mesenchymal neoplasms, accounting for approximately 20% of skin cancer (Sarver *et al.*, 2022). A recent study of 70,966 histopathological diagnoses estimates that sarcoma comprises approximately 8–15% of all canine cancers (Dell'Anno *et al.*, 2024). Canine STS encompasses over fifty distinct types with overlapping histopathological characteristics and lacks specific anatomical predilection (McSporran, 2009; Sambri *et al.*, 2021). The group of STS includes fibrosarcoma, liposarcoma, leiomyosarcoma, perivascular tumors, rhabdomyosarcoma, malignant fibrous histiocytoma, myxosarcoma, mesenchymoma, peripheral nerve sheath tumors, as well as undifferentiated sarcomas (Coindre, 2006; Bray, 2016).

The biological behavior, treatment approaches, and outcomes of canine STS are similar to those observed in humans (Bray, 2016; Gardner *et al.*, 2016; Dell'Anno *et al.*, 2024). However, the incidence of STS is significantly higher in dogs (15%) compared to humans (1%) (Liptak and Forrest, 2013; Bray, 2017). Consequently, dogs serve as a natural animal model for humans (Gardner *et al.*, 2016). Canine STS presents significant challenges in prognostic and treatment due to its heterogeneity (Liptak and Forrest, 2013). These tumors can originate from various soft tissues, resulting in diverse histological subtypes that exhibit distinct biological behaviors and therapeutic responses. This variability complicates accurate prognosis, often necessitating advanced imaging and histopathological analysis to guide treatment decisions (Bray, 2017).

Surgery is the treatment of choice for STS (Dell'Anno *et al.*, 2024). The standard surgical approach involves the excision of the tumor mass with wide margins, typically a minimum of three cm for lateral margins and one clean fascial plane for deep margins (Abrams *et al.*, 2021). However, the infiltrative nature of STS complicates surgical excision, as accurately defining tumor margins can be challenging (Bray, 2017). These difficulties increase the risk of local recurrence and distant metastasis (Dell'Anno *et al.*, 2024). Local recurrence is reported to occur in approximately 20% of cases, with a range of 7-75%, adversely affecting dogs' overall survival (Dennis *et al.*, 2011; Bray, 2017). Additional treatment should be considered depending on the STS subtype, histopathological grade, and clinical stage (Torrigiani *et al.*, 2019). Additional treatment protocols that combine surgery with adjuvant therapies, such as radiotherapy, chemotherapy, and immunotherapy, either alone or in combination, have been proposed for both humans and dogs (Dell'Anno *et al.*, 2024). Unfortunately, the effectiveness of these therapies may be limited by tumor resistance and associated side effects that need to be overcome (Liptak and Forrest, 2013).

Another challenge in canine STS is the lack of reliable prognostic indicators (Dennis *et al.*, 2011). Histopathological grading into grades 1 (low), 2 (intermediate), and 3 (high) is the most significant prognostic indicator for human STS (Coindre, 2006). A similar grading system was investigated in dogs, but no correlation between grade and incidence of metastasis, recurrence, or survival has been observed (Bray, 2016). Metastasis has been documented even in grade 1 tumors in 13% of cases (13%) (Kuntz *et al.*, 1997; McSporran, 2009). Moreover, another study on canine STS found that pretreatment biopsies underestimated the tumor's final histopathological grade in 29% of cases and overestimated it in 12% (Perry *et al.*, 2014). This challenge indicates that histopathological grading alone may be insufficient, highlighting the need for additional to complement prognostic indicators.

Additional prognostic factors have been explored, including tumor size, location, invasiveness, stage, cell proliferation, and cytogenetic markers (Dennis *et al.*, 2011). However, no clinically useful prognostic indicators have been identified to date. Existing biomarkers, such as Ki-67 and TP53, have shown promise in various canine cancers (Li *et al.*, 2015). However, their prognostic significance can differ significantly, leading to inconsistent interpretations of clinical outcomes. Common challenges that limit the evaluation of prognostic factors include biases associated with retrospective studies, small sample sizes, inconsistencies in STS classification, and the diversity of study populations (Dennis *et al.*, 2011). Establishing reliable and objective prognostic markers for predicting outcomes has become a critical concern. Additionally, the roles of cell signaling pathways require further elucidation, as their analysis may provide insights into disease activity and potential prognostic markers.

PI3K/AKT signaling pathway

This research investigates the phosphatidylinositol-3 kinase (PI3K) and protein kinase B (PKB, AKT) signaling pathways. PI3K/AKT is one of the signaling pathways contributing to cell proliferation and is a crucial regulator of various critical cellular processes such as growth, survival, and metabolism (He *et al.*, 2021; Meuten *et al.*, 2024). Activation of the PI3K/AKT pathway typically occurs in response to extracellular signals, such as growth factors binding to receptor tyrosine kinases on the cell surface. This binding initiates a cascade of signaling processes that begins with activating the PI3K enzyme (Mayer and Arteaga, 2016). This enzyme catalyzes the phosphorylation of phosphatidylinositol (4,5)-bisphosphate (PIP2) to produce phosphatidylinositol (3,4,5)-trisphosphate (PIP3), which subsequently recruits and activates AKT along with its upstream activator, 3-phosphoinositide-dependent protein kinase 1 (PDK1) (Ocana *et al.*, 2014; LoRusso, 2016). The detailed mechanism of the PI3K/AKT signaling pathway is illustrated in Figure 1.

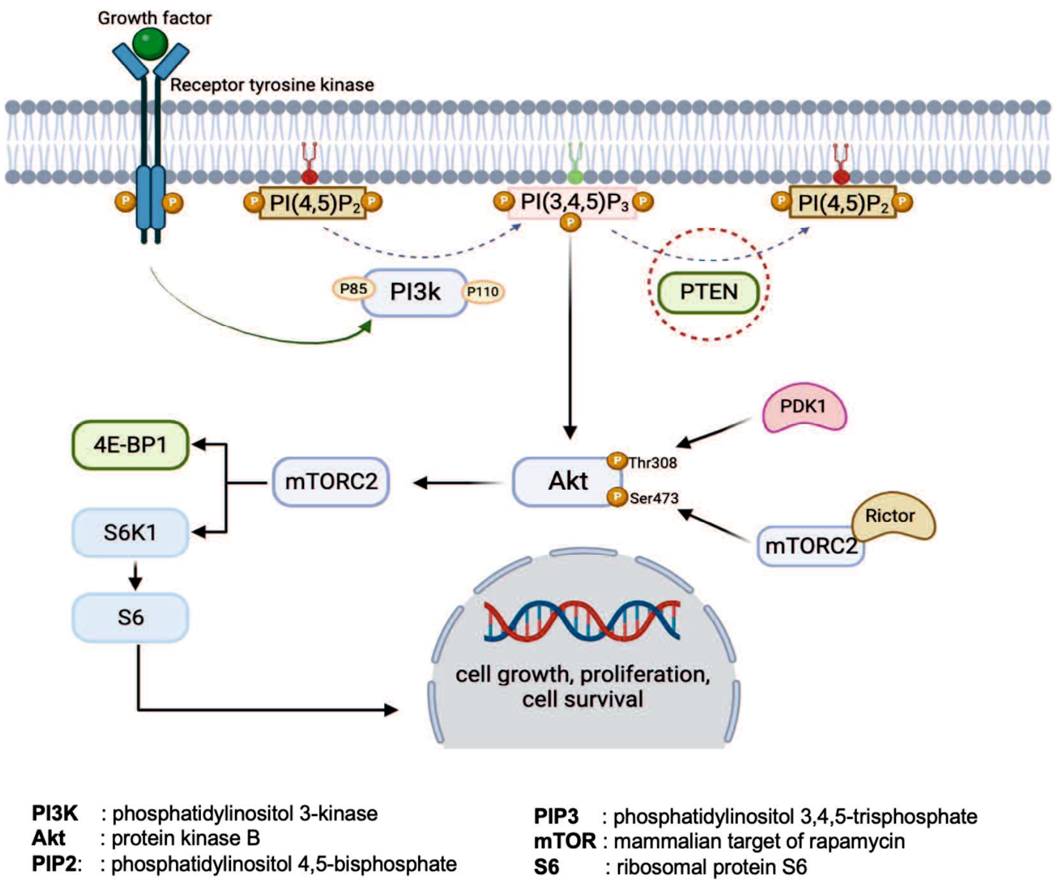

Figure 1. *Mechanism PI3K/AKT signaling pathway*

Once activated, AKT promotes cell survival and proliferation through its effects on various downstream targets, including mTOR (mechanistic target of rapamycin) and

S6K, thereby enhancing protein synthesis and cell growth (Alliouachene *et al.*, 2008; Hsieh *et al.*, 2010). The protein kinase S6K influences cell metabolism, survival, and proliferation by phosphorylating its substrate, S6, a ribosomal protein type. Consequently, the PI3K/AKT signaling pathway is crucial for maintaining cellular homeostasis and facilitating adaptive responses to extracellular stimuli (Tewari *et al*., 2022). However, dysregulation of the PI3K/AKT pathway due to genetic mutations or alterations in its components has contributed to oncogenesis and tumor progression (LoRusso, 2016; Hoxhaj and Manning, 2020). Aberrant PI3K/AKT signaling is associated with increased invasiveness, resistance to apoptosis, and poor prognosis across various cancer types, highlighting its potential target for therapeutic intervention and prognostic marker (Yu and Liu, 2022).

Our previous investigation identified the PI3K/AKT pathway activation in STS cell lines and clinical samples (Miyanishi *et al.*, 2023). The high expression of phospho-AKT, an active form of AKT, was significantly more frequent in grade 3 tumors compared to grades 1 and 2. Phospho-AKT expression was positively correlated with histopathological grade and Ki-67 index, a proliferation marker. Furthermore, elevated phospho-AKT expression was also associated with recurrence and metastasis. We confirmed that phosphorylation of AKT occurred in conjunction with S6 phosphorylation in three canine STS cell lines (MUMA-G, A72, and STS-YU1), as compared with a mouse fibroblast cell line (NIH3T3). Unfortunately, most cases in this study lacked critical clinical information relevant to prognosis, including data on metastasis, recurrence, and survival rates. Consequently, drawing definitive conclusions is challenging. Further studies and comparisons with other parameters are essential to clarify these findings and enhance our understanding of the prognostic implications.

The first chapter in this study investigated the relationship between PI3K/AKT activation and tumor-infiltrating lymphocytes (TILs), as the dysregulation of this pathway may influence TILs density within the tumor microenvironment (TME). Tumor-infiltrating lymphocytes (TILs) are immune cells, predominantly lymphocytes, that migrate from the bloodstream into the TME and infiltrate tumor tissue (Badalamenti *et al.*, 2019; Presti *et al.*, 2022; Brummel *et al.*, 2023). In cancer, TILs represent the body's immune response to tumor cells and consist mainly of various types of T cells (e.g., CD8+ cytotoxic T cells, CD4+ helper T cells, and FOXP3+ regulatory T cells), as well as some B cells and natural killer (NK) cells (Badalamenti *et al.*, 2019). Their presence, abundance, and types can indicate the ability of the immune system to recognize and potentially attack the cancer cells (Brummel *et al.*, 2023).

TILs serve as predictive markers across several cancer types (Pinard *et al.*, 2022; Presti *et al.*, 2022). However, their relevance in STS remains unclear. The composition, relative abundance, and local signaling of TILs play a pivotal role in shaping their anti-tumor or pro-tumor activity (Salgado *et al.*, 2015). The immune response's efficacy in combating cancer depends on interactions among tumor cells, stromal cells, and immune cells (Quail and Joyce, 2013). Over the past decade, TILs have demonstrated prognostic significance in canine cancer, with recent studies highlighting their potential as predictive biomarkers for immunotherapy (Badalamenti *et al.*, 2019; Loi *et al.*, 2021; Presti *et al.*, 2022). TILs contribute in various ways to modulating the anticancer immune response (Pinard *et al.*, 2022; Brummel *et al.*, 2023).

Although our previous studies have confirmed the activation of the PI3K/AKT signaling pathway, the pathogenesis of canine STS remains incompletely understood. Dysregulation of the PI3K/AKT pathway can manifest as consecutive activation, which may arise from the distinct dysregulation of individual components within this signaling cascade (Ocana *et al*., 2014). A comprehensive understanding of the PI3K/AKT signaling pathway is imperative, as each element plays a critical regulatory role in cellular functions and tumorigenesis (LoRusso, 2016; Meuten *et al.*, 2024). This underscores the necessity for comprehensive research to elucidate these aberrant mechanisms. The second chapter in this study investigates several potential major contributors to the tumorigenesis of canine STS that lead to PI3K/AKT pathway dysregulation. This information may serve as a foundation for developing therapeutic targets for STS in the future.

CHAPTER 1

The density of CD8+ tumor-infiltrating lymphocytes correlated with AKT activation and Ki-67 index in canine soft tissue sarcoma

1.1 Summary

The activation of phosphatidylinositol 3-kinase (PI3K)/AKT signaling pathway has been implicated in canine soft tissue sarcoma (STS) and may serve as a prognostic marker. This study investigated the correlation between PI3K/AKT activation in tumor cells and tumor-infiltrating lymphocytes (TILs). A total of 59 STS samples were labeled via immunohistochemistry to calculate the density of TILs, including CD3+ T cells, CD8+ T cells, CD20+ B cells, and FOXP3+ regulatory T cells. Forty-eight samples (81.3%) had intra-tumoral TILs with a high density of CD3+ T cells (mean: 283.3 cells/mm^2) and CD8+ T cells (mean: 134.8 cells/mm^2). Conversely, CD20+ B cells (mean: 73.6 cells/mm^2) and FOXP3+ regulatory T cells (mean: 9.2 cells/mm^2) were scarce. The abundance of CD3+/CD8+, CD3+/CD20+, and CD8+/CD20+ TILs were highly correlated in multivariate analyses (r=0.895, 0.946, and 0.856, respectively). Nonetheless, TILs density was unrelated to clinicopathological parameters (sex, age, tumor location, breed) and tumor grade. The abundance of CD8+ T cells was positively correlated with the activation of PI3K/AKT, indicating that samples with high levels of phospho-AKT and phospho-S6 tend to have a higher CD8+ T cell density (p=0.0032 and 0.0218, respectively). Furthermore, TILs density was correlated with the Ki-67 index, a tumor proliferation marker. Samples with a high Ki-67 index had a significantly higher abundance of CD3+ T cells, CD8+ T cells, and CD20+ B cells (p=0.0392, 0.0254, 0.0380, respectively). PI3K/AKT pathway activation may influence the infiltration of CD8+ T cells within the tumor microenvironment in canine STS.

1.2 Introduction

Tumor-infiltrating lymphocytes (TILs) have a predictive value in several cancer types (Pinard *et al.*, 2022), but their importance for canine STS is unknown. TILs composition, relative abundance, and microenvironmental signals are crucial for determining anti- and pro-tumor activity (Salgado *et al.*, 2015). Whether the immune mechanism is protective against cancer depends on the interaction between tumor cells, stromal cells, and immune cells (Quail and Joyce, 2013). Over the past ten years, TILs have demonstrated a prognostic relevance in several cancers, and recent studies have reported their potential as predictive biomarkers for immunotherapy (Badalamenti *et al.*, 2019; Loi *et al.*, 2021). However, their importance in canine STS remains unclear. TILs have a variety of roles in regulating the immune response to anticancer activity (Taddei *et al.*, 2013; Khoury *et al.*, 2018). CD8+ T cells have been associated with improved survival and lower metastasis rates (Bujak *et al.*, 2020), while CD20+ B cells enhance the humoral immune response in most cancers (Wouters and Nelson, 2018). FOXP3+-expressing regulatory T (Treg) cells are essential for preventing autoimmunity but also suppress effective anti-tumor immunity, with high Treg cells infiltration often linked to poor prognosis (Shang *et al.*, 2015).

Besides serving as prognostic markers, TILs have been associated with pathogenic characteristics and biological behavior (Carvalho *et al.*, 2011; Saeki *et al.*, 2012; Sakai *et al.*, 2018). Canine oral malignant melanoma with better survival rates had higher TILs abundance and more CD8+ T cells (Yasumaru *et al.*, 2021). In contrast, high infiltration of T cells correlated with poor prognosis in canine mammary tumors (CMT) (Saeki *et al.*, 2012). Although a high abundance of CD3+ T cells may be associated with better outcomes in histiocytic sarcoma (Lenz *et al.*, 2022), CMT patients with high CD3+ T cells have more aggressive histology and worse survival (Carvalho *et al.*, 2011). CD20+ B cells are also associated with tumor progression, metastasis, and recurrence in melanocytic tumors (Porcellato *et al.*, 2020). This contradiction indicates that the TILs profile may differ between cancer types. Therefore, it highlights the need to analyze them parallel to obtain more comprehensive information and develop prognostic tools to predict cancer behavior. Evaluating only one type of TILs may provide incomplete information about the immune environment. A new insight into prognostic indicators in canine malignancy may be obtained by determining the relationship between TILs density, proliferative markers, and signaling pathways.

To the best of the author's knowledge, the TILs profile in canine STS for prognostic purposes has not been widely reported. The prognosis of canine STS has traditionally been based on histopathological grading (Dennis *et al.*, 2011; Nyström *et al.*, 2023). However, the rate of underestimation and overestimation is 29% and 12%, respectively, when histopathological grades are determined based on pre-treatment canine STS samples obtained upon tumor resection (Perry *et al.*, 2014). Metastasis occurs even in grade 1 tumors (4/31 cases, 13%) (Kuntz *et al.*, 1997). Therefore, additional indicators are needed to predict prognosis. The PI3K/AKT signaling pathway is an essential proliferative signal in canine STS. AKT activation is correlated with a high histopathological grade and Ki-67, thus making it a potential adverse prognostic indicator (Miyanishi *et al.*, 2023).

Therefore, this preliminary study aimed to provide initial information on the potential of TILs as a prognostic indicator of canine STS by investigating the correlation of the TILs profile in canine STS with the activation of the PI3K/AKT pathway and Ki-67 index.

1.3 Material and Methods

1.3.1 Tissue samples

A total of 59 formalin-fixed paraffin-embedded (FFPE) canine STS tissues were used in this study (Supplementary Table I). The samples included 23 fibrosarcomas (FSs), 14 malignant nerve sheath tumors (MNSTs), 12 undifferentiated pleomorphic sarcomas (UPSs), six perivascular wall tumors (PWTs), two leiomyosarcomas (LMSs), one myxosarcomas (MXSs) and one liposarcoma (LPS). Tumor tissues were surgically excised from clinical cases referred to the Yamaguchi Animal Medical Centre (YUAMEC), the Veterinary Pathology Diagnostic Center (Fukuoka, Japan), and several private hospitals. Samples were collected between January, 2012, and January, 2022. Clinical data, including breed, sex, age, and tumor location, were extracted from medical records and histopathology request forms.

All samples were diagnosed based on histopathological and immunohistochemical findings by at least two veterinary pathologists. Each tissue was stained with hematoxylin and eosin (HE), followed by classification of tumor type and tumor grading (Dobromylskyj, 2022). If a diagnosis could not be made by examination of HE-stained sections alone, immunohistochemical labeling with mouse anti-desmin monoclonal antibody (D33; Dako, Glostrup, Denmark), mouse anti-vimentin monoclonal antibody (V9; Dako), mouse anti-alpha-smooth muscle actin (SMA) monoclonal antibody (1A4; Dako) and rabbit anti-S100 polyclonal antibody (Dako) was performed based on individual pathologist decisions in the diagnostic laboratory.

1.3.2 Immunohistochemistry staining

Canine STS samples were labeled via IHC to calculate the density of TILs, including CD3+ T cells, CD8+ T cells, CD20+ B cells, and FOXP3+ Treg cells. Formalin-fixed paraffin-embedded (FFPE) tissue samples were sectioned at four μm thickness and placed on glass slides. To remove paraffin wax, the sections were treated with xylene, followed by rehydration through graded ethanol solutions (100% to 70%), and finally rinsed with water. Antigen retrieval was performed using either Dako Target Retrieval Solution (pH 9, Agilent Technologies, Santa Clara, CA, US) for phospho-AKT and Ki-67; 0.01 M citrate buffer (pH 6.0) in a pressure cooker (125°C for 20 min) for TILs and phospho-S6. Endogenous peroxidase activity was blocked by incubating the slides in 3% hydrogen peroxide in phosphate-buffered saline (PBS) for 30 min. Non-specific binding was blocked with 5% skim milk and 5% bovine serum albumin (BSA) in PBS for 30 min. Slides were then incubated with primary antibodies overnight against a rat anti-CD3 monoclonal antibody (clone CD3-12, Abcam, Tokyo, Japan); rat anti-canine CD8 monoclonal antibody [clone F3- B2, own production (Sakai *et al.*, 2020)]; rabbit anti-CD20 polyclonal antibody (Thermo Fisher Scientific, Waltham, MA, USA); and mouse/rat anti-FOXP3 monoclonal antibody (clone FJK-16s, Invitrogen, Carlsbad, CA, USA) (detailed in Table 1.1).

Table 1.1 *Detailed primary antibody was used in this study.*

Protein target	Primary antibody	Origin	Dilution
Phospho-AKT	rabbit monoclonal antibody (anti-phospho AKT Ser473)	D9E (Cell Signaling Technology, Danvers, MA, US)	1:200
Phospho-S6	rabbit monoclonal antibody (anti-phospho S6 Ser235/236)	D57.2.2E (Cell Signaling Technology)	1:200
Ki-67	mouse monoclonal antibody	SolA15 (Invitrogen, Carlsbad, CA, US)	1:1000
CD3+	rat monoclonal antibody	clone CD3-12 (Abcam, Tokyo, Japan)	1:100
CD8+	rat anti-canine monoclonal antibody	clone F3- B2 (own production)	2.5 μg/ml
CD20+	rabbit polyclonal antibody	PA5 (Thermo Fisher Scientific Waltham, MA, USA)	1:100
FOXP3+	mouse/rat monoclonal antibody	clone FJK-16s (Invitrogen)	1:200

Secondary antibodies, either Histofine Simple Stain Mouse MAX PO or Rabbit MAX PO (Nichirei Bioscience, Tokyo, Japan), were applied, and detection was performed using the Peroxidase Stain DAB Kit (Nacalai Tesque, Kyoto, Japan). Isotype-matched antibody was used as a control. Finally, the sections were counterstained with Mayer's Hematoxylin Solution (Wako, Osaka, Japan) for visualization.

1.3.3 Analysis of immunohistochemistry staining

Immunohistochemistry-stained samples were scanned using a Nanozoomer 2.1 RS (Hamamatsu, Shizuoka, Japan). Subsequent analysis employed ImageJ software version 1.53 (National Institute of Health, Bethesda, MD, USA). Phospho-AKT immunoreactivity was quantified using an All-in-One Fluorescence Microscope BZ-X800 with application software (Keyence, Milton Keynes, UK). Initially, cases were classified based on two immunolabelling patterns: (1) nuclear labeling and (2) nuclear and cytoplasmic labeling. According to these categories, images were randomly obtained in five representative high-power fields (HPFs, 400x) in each section. Nuclear-only labeling was assessed as the ratio of the area of phospho-AKT-positive nuclei divided by the total nuclear area of all tumor cells. For nuclear and cytoplasmic labeling, the area of labeled cells was divided by the total area of all tumor cells to obtain the ratio of immunolabelled phospho-AKT.

Immunoreactivity for Ki-67 and phospho-S6 was assessed using the BZ-X800 microscope. To determine the area ratio of Ki67-positive nuclei, tumor hot spots exhibiting Ki-67-positive cells were identified in each slide. Images of randomly selected hot spots were captured across three representative high-power fields (HPFs, 400x magnification). The percentage of the total area of Ki-67-positive nuclei to the total nuclear area was calculated using Keyence application software. Phospho-S6 immunolabeling was classified as either positive or negative. Samples were categorized as positive phospho-S6 expression if labeling was observed in either the nuclei or cytoplasm.

The TILs-stained samples were scanned using Nanozoomer 2.0 RS and analyzed using ImageJ software ver. 1.53. TILs density was evaluated using semi-quantitative calculations. Positive immunolabel cells in the intratumoral area were counted in one mm^2 from ten independent hotspot areas at high-power representative microscopic fields (HPFs, 0.0625 mm^2), as illustrated in Supplementary Figure I. Dense aggregates of lymphocytes that were reminiscence of tertiary lymphoid structures were excluded. Since the cut-off value was not standardized, the mean was used to obtain TILs density/mm^2. TILs density was then associated with phospho-AKT and phospho-S6 as the major indicators of PI3K/AKT pathway activation, as well as the Ki-67 index. Tumor cells were classified as high phospho-AKT (samples in the upper quartile) or low phospho-AKT (the remaining samples) according to the average ratio of positive immunolabeled cells. A similar procedure was also used for classifying the Ki-67 index. Further, phospho-S6 was categorized as positive or negative according to immunolabeling.

1.3.4 Statistical analysis

TILs density was compared with the clinicopathological parameters using ANOVA or Fisher's exact test, depending on the sample sizes. A non-parametric Wilcoxon test was used to compare TILs density with phospho-AKT and phospho-S6 expression. Multivariate analysis with the Pearson correlation test was performed to determine whether there is a correlation between the subset TILs. Finally, a nonparametric Wilcoxon test was also conducted to compare the CD8+/FOXP3+ ratio to the Ki-67 index. *P*-values less than 0.05 were considered to indicate statistical significance. All statistical tests were performed using JMP Pro Software version 15 (SAS Institute, Tokyo, Japan).

1.4 Results

1.4.1 Patient demographic

In this study, 59 canine soft STS samples were obtained from several institutions (Supplementary Table I). Several samples had incomplete information. Of the 48 TILs-positive samples, 27 were male dogs (56.2%), and 21 were female dogs (43.8%), with ages ranging from 5-17 years (median: 11 years; interquartile range=10-13 years). Tumors were predominantly located on the extremities, with 35.8% identified on the upper limb (19/53) and 30.2% on the hind limb (16/53). Additional tumor locations included the thorax-abdominal region (15.1%), head and neck area (13.2%), and internal organs (5.7%). Breed data was discernible in 40 dogs, with small breeds representing 50% (20/40), while medium and large breeds accounted for 22.5% and 27.5%, respectively. Samples from mixed breeds were excluded from breed-based analysis. The grade distribution of the 59 STS samples was nearly uniform, with 33.9% categorized as grade 1 (n=20), 33.9% as grade 2 (n=20), and 32.2% as grade 3 (n=19).

1.4.2 TILs profiles

Of the 59 analyzed samples, 48 (81.3%) exhibited TILs with variable densities (Supplementary Table I). The densities for CD3+, CD8+, CD20+, and FOXP3+ TILs were 283.3±55.5/mm^2(range=0-2,100/mm^2), 134.8±30.8/mm^2 (range=0-936/mm^2), 73.6±1.57 /mm^2 (range=0-635/mm^2), and 9.2±2.2/mm^2 (range=0-91/mm^2), respectively. No significant differences in TILs profiles were observed concerning clinicopathological parameters, including sex (male *vs*. female), age (<11.3 *vs*. ≥11.3 years), tumor location, or dog breeds (small, medium, and large). However, an unpaired comparison revealed a statistical difference in FOXP3+ density across STS subtypes (p=0.016). Table 1.2 compares TILs density and grades to identify any histopathological discrepancies.

Generally, no significant differences were found in the abundance of CD3+, CD8+, CD20+, and FOXP3+ TILs across tumor grades. In multivariate analysis, correlations were classified as strong (score: 0.7-1.0), moderate (0.5-0.7), and low (<0.5). Results indicated a strong correlation between CD3+/CD8+ (*r*=0.895), CD3+/CD20+ (*r*=0.946), and CD8+/CD20+ (*r*=0.856) (Figure 2.1).

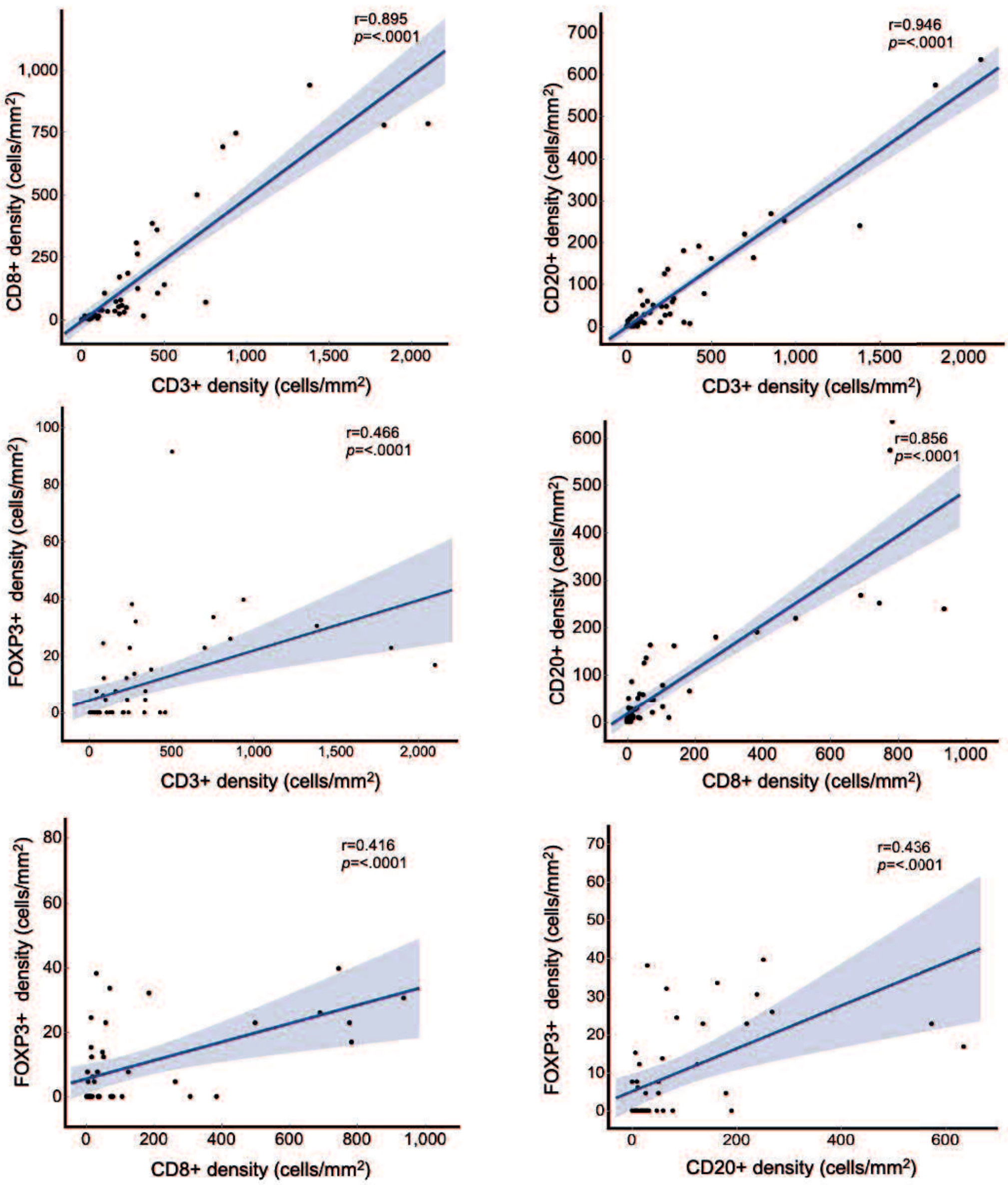

Figure 2.1 *Multivariate analyses of the relationship of the density of different tumor-infiltrating lymphocytes (TILs) subtypes: CD3+ T cells, CD8+ T cells, CD20+ B cells, and FOXP3+ Treg cells (Pearson correlation test, p=0.05).*

In contrast, a low correlation was observed between CD3+/FOXP3+ (*r*=0.466), CD8+/FOXP3+ (*r*=0.416), and CD20+/FOXP3+ (*r*=0.436) densities.

The PI3K/AKT pathway is activated in canine STS (Miyanishi *et al.*, 2023). Considering that TILs may serve as a prognostic indicator in canine STS, this study investigated the potential correlation between TILs density and phospho-AKT as a PI3K/AKT pathway activation marker. Results indicated that average densities of CD3+, CD8+, CD20+, and FOXP3+ TILs in the low versus high phospho-AKT group were as follows: 230.2 *vs*. 338.2 (*p*=0.0174); 76.4 *vs*. 197.4 (*p*=0.0032); 62.2 *vs*. 86.8 (*p*=0.0268); and 8.9 *vs*. 9.6 (*p*=0.885), respectively (Figure 2.2).

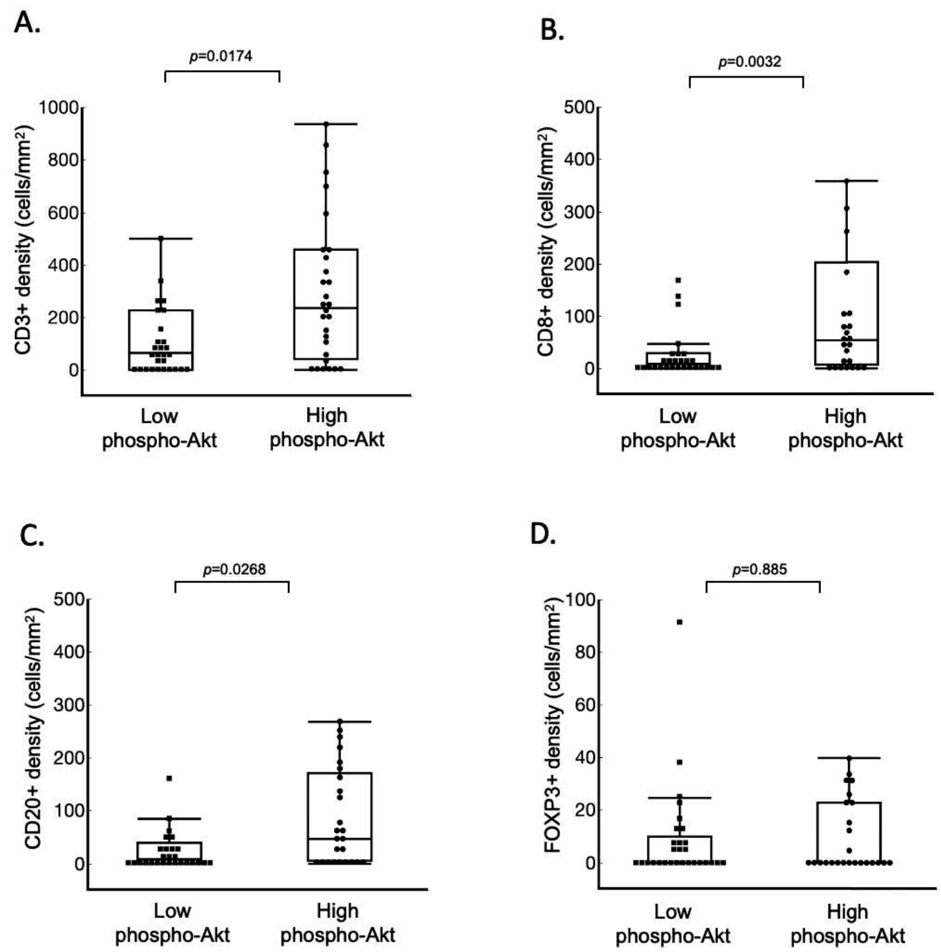

Figure 2.2. *Comparison of tumor-infiltrating lymphocytes (TILs) density (cells/mm^2) and phospho-AKT (high expression, n=29 vs. low expression, n=30). A) CD3+ T cells; B) CD8+ T cells; C) CD20+ B cells; D) FOXP3+ Treg cells (Wilcoxon test, p=0.05).*

The activation of the PI3K/AKT pathway led to the activation of mTOR, which phosphorylated the ribosomal protein S6 kinase (S6K1) and its substrate, ribosomal S6 proteins (S6) (Meuten *et al.*, 2024). To further explore any potential correlation between TILs and the PI3K/AKT pathway, TILs densities were compared between phospho-S6-expressing and non-expressing groups. Nonparametric analyses indicated that samples expressing phospho-S6 tended to have a higher TILs density. The comparison of TILs density in negative *versus* positive phospho-S6 samples was as follows: CD3+ T cells, 269.1 *vs*. 285.9 (p=0.068); CD8+ T cells, 100 *vs*. 147 (p=0.0218); CD20+ B cells, 74.6 *vs*. 70.5 (p=0.0757); and FOXP3+ Treg cells, 5.5 *vs*. 11.7 (p=0.3137). Only the abundance of CD8+ T cells showed a statistically significant difference, while others did not (Figure 2.3).

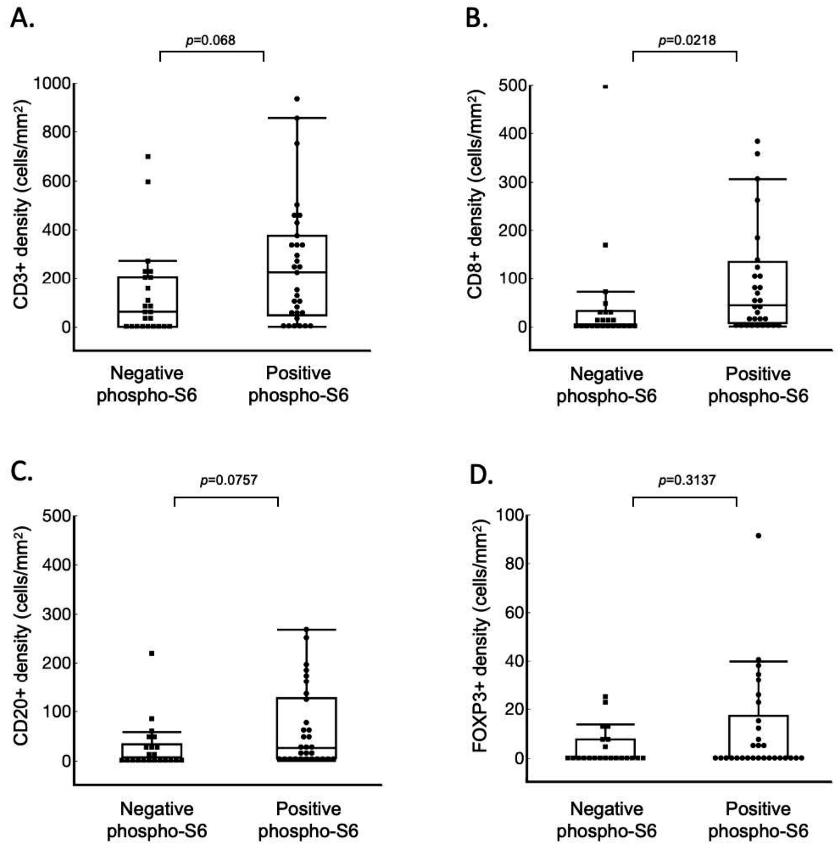

Figure 2.3. *Comparison of tumor-infiltrating lymphocytes (TILs) density (cells/mm^2) and phospho-S6 staining (positively immunolabeled, n=45 vs. negatively immunolabeled, n=11). A) CD3+ T cells; B) CD8+ T cells; C) CD20+ B cells; and D) FOXP3+ Treg cells (Wilcoxon test, p=0.05).*

Table 1.2 *Comparison of tumor-infiltrating lymphocytes (TILs) density to clinicopathological parameters*

Parameter	n (%)	CD3+ TILs density (cells/mm^2)			CD8+ TILs density (cells/mm^2)			CD20+ TILs density (cells/mm^2)			FOXP3+ TILs density (cells/mm^2)		
		mean	range	*p*-value	mean	range	*p*-value	mean	range	*p*-value	mean	range	*p*-value
Sex													
Male	27 (56.2)	286 ± 417	0-1833	0.731	141 ± 240	0-776	0.722	71 ± 129	0-574	0.747	10 ± 21	0-91	0.328
Female	21 (43.8)	258 ± 317	0-1382		112 ± 217	0-936		55 ± 72	0-239		9.5 ± 12	0-38	
Age													
< 11.3	25 (48.1)	291 ± 271	0-935	0.162	127 ± 202	0-744	0.473	71 ± 81	0-268	0.237	14 ± 21	0-91	0.137
≥ 11.3	27 (51.9)	310 ± 560	0-2100		153 ± 272	0-936		84 ± 168	0-635		6.3 ± 10	0-32	
Tumor location													
Upper limb	19 (35.8)	344 ± 613	0-2100		165 ± 282	0-782		109 ± 194	0-635		7.3 ± 11	0-39	
Hind limb	16 (30.2)	257 ± 365	0-1382		135 ± 272	0-936		62 ± 83	0-268		9.3 ± 12	0-32	
Head-neck	7 (13.2)	293 ± 227	33-595	0.636	147 ± 209	3-469		14 ± 14	0-28.9	0.689	15 ± 16	0-38	0.688
Thorax-abdomen	8 (15.1)	291 ± 256	0-752		109 ± 126	0-383	0.789	69 ± 78	0-190		5.9 ± 12	0-33	
Others	3 (5.7)	312 ± 267	123-501		83 ± 52	36-138		80 ± 73	19-161		30 ± 53	0-91	
Breed													
Small	20 (50.0)	383 ± 486	0-2100		150 ± 225	0-782		87 ± 152	0-635		12 ± 22	0-91	
Medium	9 (22.5)	324 ± 596	0-1833	0.835	110 ± 271	0-776	0.432	84 ± 199	0-574	0.743	4.4 ± 8.6	0-22	0.371
Large	11 (27.5)	238 ± 277	0-935		146 ± 235	0-744		73 ± 91	0-251		12 ± 15	0-39	
STS type													
Fibrosarcomas	21 (35.6)	173 ± 192	0-699		111 ± 172	0-498		43 ± 66	0-219		6.2 ± 10	0-38	
MNST	16 (27.1)	366 ± 578	0-2100		148 ± 294	0-936		93 ± 170	0-635		7.0 ± 11	0-30	
UPS	12 (20.3)	302 ± 551	0-1833	0.351	147 ± 289	0-776	0.701	85 ± 169	0-574	0.871	6.2 ± 12	0-39	**0.016**
PWT	6 (10.2)	276 ± 313	0-855		207 ± 257	0-689		91 ± 109	0-268		12 ± 14	0-32	
Others	4 (6.8)	433 ± 269	0-752		65 ± 54	13-138		85 ± 90	0-163		35 ± 40	0-91	
Grade histopathology													
Grade 1	20 (33.9)	179 ± 168	0-595		61 ± 90	0-306		38 ± 51	0-180		4.9 ± 11	0-38	
Grade 2	20 (33.9)	362 ±601	0-2100	0,404	171 ± 261	0-782	0.254	107 ± 191	0-635	0.285	13 ± 22	0-91	0.358
Grade 3	19 (32.2)	308 ± 396	0-1382		170 ± 293	0-936		73 ± 98	0-268		9.5 ± 14	0-39	

TILs: tumor-infiltrating lymphocytes; MNST: malignant nerve sheath tumor; UPS: undifferentiated pleomorphic sarcoma; PWT: perivascular wall tumor

1.4.3 TILs density and its correlation with prognostic relevance

A nonparametric statistical analysis was performed to determine the relationship between TILs density and the Ki-67 label index present in tumor cells. The results demonstrated a positive correlation between TILs density and the Ki-67 index. Samples with a high Ki-67 index exhibit significantly higher densities of CD3+, CD8+, and CD20+ TILs within the tumor microenvironment. The comparisons of TILs densities in the low *versus* high Ki-67 index group were as follows: CD3+ T cells, 185.8 *vs*. 384.3 cells/mm^2 (p=0.0392); CD8+ T cells, 74.9 *vs*. 194.7 cells/mm^2 (p=0.0254); CD20+ B cells, 43.2 *vs*. 104.1 cells/mm^2 (p=0.0380); and FOXP3+ Treg cells, was 6.0 *vs*. 12.0 cells/mm^2 (p=0.1630) (Figure 2.4). Furthermore, the CD8+/FOXP3+ ratio in low *vs*. high Ki-67 index samples was 12.5 *vs*. 16.2 cells/mm^2 (p=0.0413).

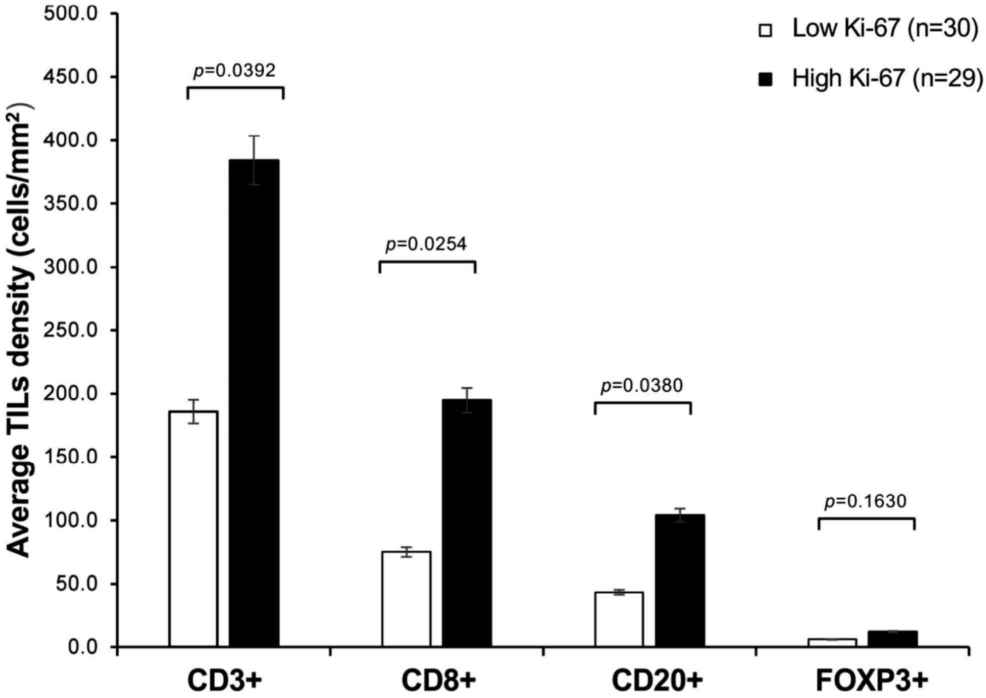

Figure 2.4. *Analysis of tumor-infiltrating lymphocytes (TILs) density compared to labeled Ki-67 index (high Ki-67, n=29 vs. low Ki-67, n=30). The samples were grouped into two: the Ki-67 index was above the mean (black chart) and below the mean (white chart) (Wilcoxon test, p=0.05).*

1.5 Discussion

In this study, 81.3% of the canine STS samples exhibited lymphocyte infiltration, with T cells likely more dominant than B cells. The composition was dominated by CD3+ and CD8+ T cells. Conversely, Treg and B cells were infrequent and randomly scattered across a large area. The high infiltration of CD3+ and CD8+ T cells, combined with low levels of FOXP3+ Treg cells, initially indicated a favorable immune response in STS. Judge *et al*. (2022) reported that human STS patients with high TILs densities experience improved survival rates. The TILs profiles observed in the present study exhibit similarities to those found in human STS. A recent study indicated that human STS typically tended to have a low immuno-suppressive TME, identical to the low density of FOXP3+ Treg cells (Chalmers *et al.*, 2017). Furthermore, the low percentage of CD20+ B cells aligns with data from human STS, where they are also infrequently encountered, present in only 14% of samples (Nyström *et al.*, 2023).

This study indicated that TILs density was not significantly correlated with clinicopathological parameters or histopathological grades. Nonetheless, a high-grade canine STS tended to be associated with an increased likelihood of lymphocyte infiltration. Thus, TILs density may be case-dependent, even among tumors of the same grade. However, these findings somewhat differ from a previous canine STS study that reported that older age, high histopathological grade, and boxer breeds are negative prognostic indicators (Chiti *et al.*, 2021). These discrepancies may be due to the limited sample size in each study. In the present study, the numbers of FOXP3+ Treg cells varied between STS subtypes in univariate analysis but lost significance in multivariate models. This observation affirms that canine STS patients exhibit increased peripheral Treg cells levels compared to healthy dogs (Burton *et al.*, 2011).

In the current investigation, TILs exhibited a positive correlation with PI3K/AKT activation. The group characterized by high levels of phospho-AKT and positive phospho-S6 demonstrated a tendency for increased TILs density. While only CD8+ T cells had statistically significant differences, the average densities of CD3+ T cells, CD20+ B cells, and FOXP3+ Treg cells also elevated in the PI3K/AKT-activated group. Enhanced PI3K/AKT signaling pathway in cancer cells may influence T cells density through complex mechanisms depending on various factors (Mafi *et al.*, 2022). The PI3K/AKT pathway orchestrates an adaptive immunity by facilitating T-cell activation, modulating the balance between Treg and Th17, and influencing metabolic programming (Rao *et al.*, 2010; Powell *et al.*, 2012; Hawkins and Stephens, 2015).

This study's result are in line with previous research (Sobral-Leite *et al.*, 2019), which observed increased TILs densities in breast cancer with elevated PI3K/AKT phosphorylation. Activation of the PI3K/AKT pathway can promote the secretion of some chemokines, such as CCL2, CCL5, and CXCL10, which are known to attract and enhance T cells infiltration (So and Fruman, 2012). In addition, the PI3K/AKT pathway influences the expression of adhesion molecules such as intercellular adhesion molecule 1 (ICAM-1) (Haydinger *et al.*, 2023) and vascular cell adhesion molecule 1 (VCAM-1) (Kong *et al.*, 2018). These adhesion molecules interact with their corresponding receptors on the T cells, further facilitating their infiltration into TME (Amin *et al.*, 2006).

Histopathological grading and Ki-67 immunolabeling have been used as prognostic indicators of canine STS (Dennis *et al.*, 2011). Elevated Ki-67 levels in cancer cells suggest an increased proportion of actively proliferating tumor cells. In this study, a high Ki-67 index was significantly correlated with a high TILs density within TME, suggesting an appropriate lymphocyte response against STS through intratumoral and tumor nest infiltration. Similarly, Mitchell *et al.* (2019). reported that in human non-small cell lung cancer, a high Ki-67 index was associated with increased infiltration of increased infiltration of CD3+, CD4+, CD8+, CD45RO+, and FOXP3+ Treg cells.

The precise mechanistic pathways underlying this correlation remain elusive, and uncovering the accurate mechanisms represents another critical challenge that warrants future investigation. It is hypothesized that this relationship may related to the high proliferation rate of cancer cells, potentially leading to an increased production of tumor-associated antigens. Since the rapid proliferation of tumors is associated with a high inflammatory response (Greten and Grivennikov, 2019), this correlation might be due to a more robust immunogenic profile in highly proliferating tumors, thereby promoting T-cell activation and infiltration.

The correlation between TILs density and the PI3K/AKT pathway in cancer cells is complex, involving the interplay of cytokines, chemokines, and growth factors. Reciprocal signaling between cancer cells and other components within TME may play a critical role in promoting or inhibiting anticancer immune response.

CHAPTER 2

Potential contribution of epidermal growth factor receptor to PI3K/AKT pathway dysregulation in canine soft tissue sarcoma

2.1 Summary

The previous studies identified activation of the phosphatidylinositol-3 kinase (PI3K)/ protein kinase B (PKB, AKT) pathway in canine STS cell lines and clinical samples, but the underlying mechanism remains unclear. This study investigated PTEN loss, *PIK3CA* mutation, and EGFR over-expression as potential drivers of PI3K/AKT pathway activation in canine STS. Thirty-six STS samples were analyzed. PTEN and EGFR expression were evaluated using immunohistochemistry, while *PIK3CA* and *EGFR* mutations were assessed through DNA sequencing. PTEN was expressed in all analyzed samples with no evidence of loss. Weak PTEN expression was observed in 33.3% of samples, while 66.7% showed normal expression. DNA sequencing of *PIK3CA* revealed a single point mutation (c.554 A>C, H554P) in one case, but no hotspot mutations were identified. High EGFR expression was significantly correlated with elevated phospho-AKT levels ($p<0.0001$). Immunolabelling indicated that 30 samples (83.3%) were EGFR-positive, and 27 of these also showed positive phospho-AKT labeling. Accordingly, one missense point mutation in exon 21 of *EGFR* (E868K) was identified in one of 12 samples. EGFR over-expression, rather than PTEN loss or *PIK3CA* mutations, may contribute to PI3K/AKT pathway dysregulation in canine STS.

2.2 Introduction

Soft tissue sarcomas (STS) originate from mesenchymal cells and are commonly found in dogs' cutaneous and subcutaneous tissue (Dobromylskyj, 2022). In addition to encompassing various histological phenotypes, these cancers are considered a group based on their similarity in clinical and histopathological features (Pillozzi *et al.*, 2021). The pathogenesis of canine STS remains incompletely elucidated, and investigation into cell signaling pathways might yield crucial insight. In previous research, we identified activation of the phosphatidylinositol-3 kinase (PI3K)/protein kinase B (PKB, AKT) pathway on STS cell lines and clinical samples (Miyanishi *et al.*, 2023). The PI3K/AKT signaling pathway controls various cellular activities, including growth, proliferation, survival, and metabolism (Hoxhaj and Manning, 2020; Meuten, Dean, and Thamm, 2024). The complex canonical PI3K/AKT cascade features numerous initiation, regulatory, and effector sites (Guerra *et al.*, 2021; Yu, Wei and Liu, 2022).

Upon activation, AKT phosphorylates numerous downstream targets involved in essential cellular processes (Ocana *et al.*, 2014; Meuten, Dean and Thamm, 2024). In contrast, the phosphatase and tensin homolog deleted on chromosome 10 (PTEN) hinders AKT's activation and functioning as a tumor suppressor (Stefano and Giovanni, 2019). Dysregulation in the PI3K/AKT signaling pathway has been implicated in tumorigenesis (Campos *et al.*, 2014; Lorch *et al.*, 2019; Asproni *et al.*, 2021; Kim *et al.*, 2021). PI3K/AKT dysregulation can be indicated by consecutive activation, which can arise through the distinct dysregulation of individual components of this signaling cascade (Porta, Paglino, and Mosca 2014). These aberrations can occur due to mutations in the *PI3K* or *AKT* genes, loss of PTEN, or continuous activation of the upstream cascade (Dobashi *et al.*, 2009; Porta, Paglino and Mosca, 2014). Mutation of the *PIK3CA gene*, which encodes the p110α catalytic subunit of phosphatidylinositol 3-kinase, has been reported as the second most common mutation in human cancer (Lee *et al.*, 2019). This mutation has been demonstrated to induce the hyperactivation of the PI3K/AKT signaling pathway (Choy *et al*., 2012; Estabrooks *et al*., 2023).

Loss of PTEN results in the uncontrolled regulation of AKT levels, which promotes the PI3K/AKT pathway hyperactivation, thus leading to tumorigenesis (Bazzichetto *et al.*, 2019; Weng *et al.*, 2020). PTEN is frequently subject to mutations, deletions, or down-regulation in different types of canine cancer (Meuten, Dean, and Thamm, 2024). Another factor that potentially contributes to PI3K/AKT dysregulation is the increased activity of the upstream cascade, especially the receptor tyrosine kinase (RTK) (Hoxhaj and Manning 2020; Porta, Paglino, and Mosca 2014). One extensively studied RTK upstream of PI3K/AKT signaling is the epidermal growth factor receptor (EGFR, also known as HER-1 or ErbB-1) (Gori *et al.*, 2009). Over-expression and mutation of EGFR have been associated with a more aggressive malignant phenotype characterized by increased resistance to therapeutic modalities and worse clinical outcomes (Selvarajah *et al.*, 2012; Shan *et al.*, 2017).

The precise mechanism underlying consecutive activation of the PI3K/AKT signaling pathway in canine STS remains elusive. Therefore, it is necessary to use the insights from human medicine to address this knowledge gap. A comprehensive understanding of the PI3K/AKT signaling pathway is imperative, as each component exerts distinct and pivotal regulatory roles in cellular functions and tumorigenesis. This situation emphasizes the underscoring for comprehensive research to elucidate these aberrant mechanisms. This study explored several PI3K/AKT aberrations, including PTEN loss, *PIK3CA mutation*, and EGFR over-expression, as potential major contributors to the tumorigenesis of canine STS.

2.3 Materials and Methods

2.3.1 Tissue samples

Tissue samples from 43 canine STS cases utilized in prior studies were used in this study (Supplementary Table II). The hospital database collected archival clinical data on patient information, tumor grade, and clinical history. Tissue samples were preserved in 4% neutral buffered formalin, embedded in paraffin, sectioned at four µm thickness, and stained with hematoxylin-eosin (HE). Subsequently, two veterinary pathologists classified the tumor type and determined the tumor grades. If a conclusive diagnosis could not be determined with HE staining, immunohistochemical (IHC) labeling was conducted. This IHC procedure utilized the following antibodies: mouse anti-desmin monoclonal antibody (D33; Dako, Glostrup, Denmark), mouse anti-vimentin monoclonal antibody (V9; Dako), mouse anti-alpha-smooth muscle actin (SMA) monoclonal antibody (1A4; Dako), and rabbit anti-S100 polyclonal antibody (IR504, Dako). Tumors were identified according to the World Health Organization (WHO) classification for cancers in domestic animals (Misdorp, 1976). The histological grading system was designed using criteria such as tumor differentiation, mitotic index, and tumor necrosis (Dobromylskyj, 2022).

2.3.2 Immunohistochemistry staining

Immunostaining for PTEN and EGFR was performed on 36 samples, as some FFPE samples had incurred damage. Briefly, four µm-thick tissue sections were deparaffinized in xylene to remove paraffin and then gradually rehydrated using a sequence of different concentrations of alcohols, ultimately ending with distilled water. Antigen retrieval was performed using Dako Target Retrieval solution, pH 9 (Agilent Technologies, Santa Clara, CA, USA) in an autoclave (121℃, 20 min) for PTEN staining and in Histofine Protrease solution (Nichirei Bioscience, Tokyo, Japan) at room temperature for 6 min for

EGFR staining. The sections were subsequently immersed in a solution of 3% H_2O_2 in phosphate-buffered saline (PBS) for 30 min to inhibit endogenous peroxidase activity. Afterwards, the slides were incubated with 5% skim milk and 5% bovine serum albumin (BSA) in PBS for 30 min. Slides were incubated with primary antibodies against rabbit anti-PTEN monoclonal antibody (138G6, 1:200; Cell Signaling Technology, Danvers, MA, USA) and mouse anti-EGFR monoclonal antibody (31G7, Nichirei Bioscience). They were then incubated overnight at 4°C. Rabbit IgG antibody (DA1E; Cell Signaling Technology) and mouse IgG_1 antibody (P3.6.2.8.1; eBioscience, Waltham, MA, USA) were utilized as negative controls. The samples were then incubated with secondary antibodies using Histofine Simple Stain Mouse MAX PO (Nichirei Bioscience) or Histofine Simple Stain Rabbit MAX PO (Nichirei Bioscience). The sections were visualized using a peroxidase staining diaminobenzidine kit (Nacalai Tesque, Kyoto, Japan) and counterstained with Mayer's Hematoxylin Solution (Wako, Osaka, Japan). Phospho-AKT staining was conducted as in previous work (Miyanishi *et al.*, 2023).

2.3.3 Immunohistochemistry analysis

PTEN and EGFR-stained samples were scanned using a Nanozoomer 2.1 RS (Hamamatsu, Shizuoka, Japan). Subsequent analysis employed ImageJ software version 1.53 (National Institute of Health, Bethesda, MD, USA). The program enabled examination at low (100x) and high (200x or 400x) magnifications. The levels of phospho-AKT immunoreactivity were measured using an All-in-One Fluorescence Microscope BZ-X800 (Keyence, Osaka, Japan) alongside its dedicated application software. PTEN expression levels were assessed using the Allred scoring method with minor modifications (Gaber *et al*. 2014; Mundhenk *et al*. 2011). This method evaluates both the proportion of positive cells and the intensity of immunolabeling. The proportion of positive cells was categorized according to the following scale: *0*: negative; +*1*: ≤10% positive cells; +*2*: 11-49% positive cells; and +*3*: ≥50% positive cells. The intensity of immunolabelling was assessed following this scale: *0*: negative; +*1*: weak intensity; +*2*: strong intensity. The final PTEN expression levels combine the scale of positive cell percentage and the immunolabelling intensity across all examined fields, resulting in five possible final scores. Total final scores of *0* and *1* are categorized as "negative," scores of *2* and *3* as "weak expression," and scores of *4* to *5* as "normal expression". A similar method was employed to evaluate EGFR with the expression levels categorized as negative, weak, moderate, and strong expression categories (Cho *et al*., 2021; Gaber *et al*., 2014). Supplementary Figure II displays the representative results of the immunolabeling scoring for EGFR and PTEN.

2.3.4 Mutation analyses of PIK3CA and EGFR

DNA sequencing was performed to determine the existence of mutations in the *PIK3CA* and *EGFR* genes. 16 samples were subjected to DNA sequencing due to either amplification failures or limited tumor samples. Genomic DNA was extracted from FFPE samples using the QIAamp DNA FFPE Tissue kit (Qiagen, Tokyo, Japan) according to the manufacturer's instructions. Using this genomic DNA as a template, the individually targeted exons were amplified using MightyAmp DNA polymerase Ver.3 (Takara Bio Inc, Shiga, Japan), and the primers are shown in Table 2.1. The DNA sequencing of the *PIK3CA* gene targeted exons 10 and 21, whereas that of *EGFR* gene expression exons 18, 19, 20, and 21, as reported in various other canine cancer studies. PCR conditions were denaturing at 98℃ for 2 min, followed by 40 cycles of 98℃ for 10 s, 60℃ for 15 s, and 68℃ for 30 s. The expected sizes of amplified products were obtained from the gel following agarose electrophoresis. Each sequence was confirmed by Sanger sequence analysis and compared with genomic sequences of *PIK3CA* and *EGFR* in the GenBank database (accession numbers LC625864.1 and LC643766.1, respectively).

Table 2.1. *Primers used for amplifying and sequencing PIK3CA and EGFR genes*.

Target Gene	Exon location	Name	Nucleotide sequences	Product size	Reference
PIK3CA	Exon 10	YTM2531	5'- TTCGCCATTTTCTCTTTTTGTAGA -3'	300bp	Lee *et al*., 2019
		YTM2532	5'- AGGTATGGTAAAACCTGCAAGATA -3'		
	Exon 22	YTM2533	5'- TGTGACATTTGAGCAGAGACC -3'	384 bp	Own designed
		YTM2534	5'- TCCAGATAATGAGCTTTCGGTT -3'		
EGFR	Exon 18	YTM2519	5'- GCAGTTGCTCTTCCTTGTCT -3'	252 bp	Cho *et al*., 2021
		YTM2520	5'- CAACACAGAGTAGACGAGGC -3'		
	Exon 19	YTM2521	5'- AGTCCGTCTATCTCACGAGG -3'	212 bp	Cho *et al*., 2021
		YTM2522	5'- GTGGACAAGCAGAGGACAAA -3'		
		YTM2629	5'- GGGCTTCTCTGAAGCTTTCC -3'	285 bp	Own designed
		YTM2630	5'- GGAGCAGCGAGCGAAGTA -3'		
	Exon 20	YTM2523	5'- CTCTCCCCTTCTTCTTCCCA -3'	336 bp	Cho *et al*., 2021
		YTM2524	5'- TTATTTCTCCCCCTTGCTGC -3'		
	Exon 21	YTM2525	5'- GGTGTGAACAGGACATGGG -3'	326 bp	Cho *et al*., 2021
		YTM2526	5'- TTCTGAGAACGTCCCCTAGG -3'		

2.3.5 Statistical analysis

The statistical tests were performed using JMP Pro Software version 15 (SAS Institute, Tokyo, Japan). The non-parametric Wilcoxon test was used to compare EGFR and PTEN expression levels against the phospho-AKT area ratio. Fisher's exact test was used to evaluate the expression levels of EGFR and PTEN in relation to clinicopathologic parameters. A multivariate analysis using the Pearson correlation test was performed to ascertain whether there is a correlation between EGFR, PTEN, *PIK3CA* mutation, and any other clinicopathological parameter. *P-values* below 0.05 were considered to indicate statistical significance.

2.4 Results

2.4.1 PTEN was intact in canine STS

IHC analysis demonstrated intact PTEN expression in all 36 samples (100%), without any cases of PTEN loss detected. Among these, 12 out of 36 samples (33.3%) exhibited weak PTEN expression, while 24 out of 36 samples (66.7%) showed normal PTEN levels. The weak PTEN expression group displayed a higher mean phospho-AKT area ratio than the group with normal PTEN expression (p=0.0433, as shown in Figure 3.1A). However, the linear regression analysis did not reveal a significant correlation (p=0.0552, Figure 3.1B). These findings suggest that AKT activation in canine STS may occur independently of PTEN loss.

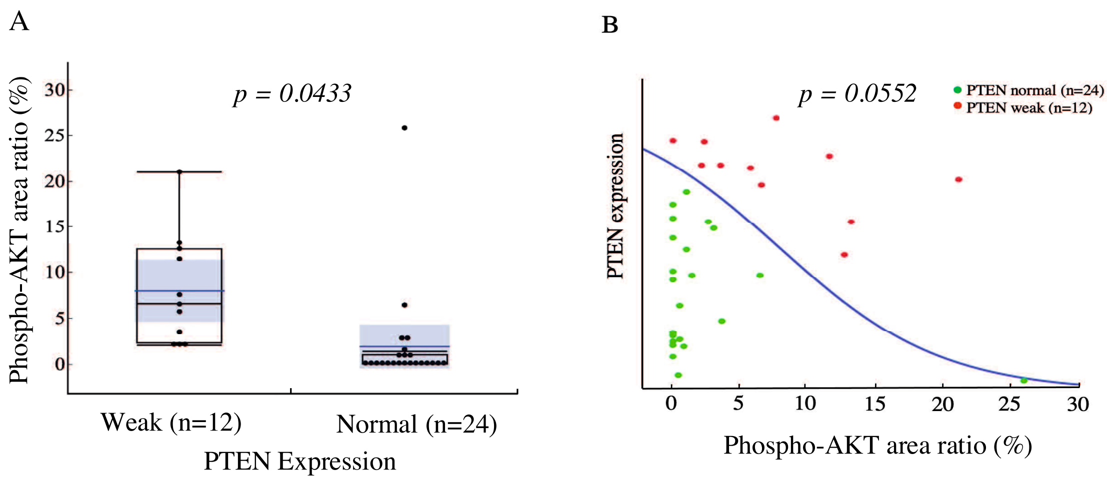

Figure 3.1. *Comparison of PTEN expression scores with phospho-AKT area ratio. A) The phospho-AKT area ratio in the PTEN weak group (n=12) compared to the normal PTEN group (n=24) (p=0.0433). B) The correlation between PTEN score and phospho-AKT area ratio based on simple logistic regression (p=0.0552).*

2.4.2 Mutation on PIK3CA and EGFR

In this study, 2 out of 16 (12.5%) sequenced STS samples exhibited a point mutation, each in exons 10 and 21 of the *PIK3CA* gene. The point mutation in exon 10 was located at nucleotide 554 A>C (H554P). The other sample demonstrated the nonsense mutation c.1661 G>A (E1661K). Analysis of the *EGFR* gene revealed one out of 12 sequenced samples (8.3%) had a mutation in exon 21, while no mutations were found in exons 19 and 20. This *EGFR* mutation in exon 21 is located at nucleotide 868 G>A (E868K). In addition, two samples exhibited nonsense EGFR mutations, with one mutation located in exon 18 and the other in exon 21.

2.4.3 EGFR expression correlated with phospho-AKT

In total, 30 out of 36 (83.3%) exhibited positive EGFR immunolabeling. Of them, 38.8% showed weak EGFR expression, while the remaining 44.4% samples displayed moderate to high EGFR expression. Of the 30 samples positive for EGFR immunolabeling, 27 also showed positive immunolabeling for phospho-AKT. Remarkably, the six samples with strong EGFR expression had elevated phospho-AKT area ratio, suggesting an initial indication of EGFR as an upstream activator of the PI3K/AKT pathway. Next, I analyzed the relationship between EGFR expression and phospho-AKT levels. EGFR expression was categorized into four groups: negative, weak, moderate, and strong. The group characterized by strong EGFR immunolabeling exhibited a significantly higher phospho-AKT area ratio than the other groups (p<0.0001, Figure 3.2 A).

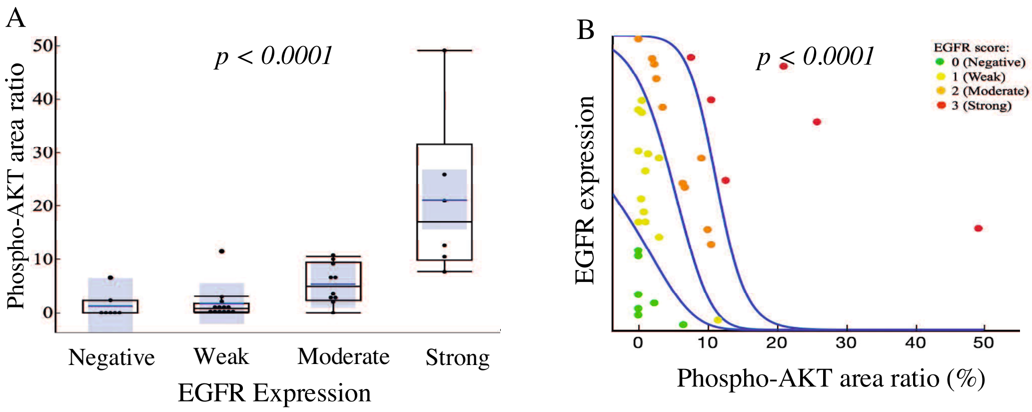

Figure 3.2 *Comparison of EGFR expression scores with phospho-AKT area ratio. A) The mean phospho-AKT area ratio among EGFR groups (p<0.0001). B) The positive correlation between EGFR score and phospho-AKT area ratio based on simple logistic regression (p<0.0001).*

Additionally, linear regression analysis revealed a positive association between EGFR expression levels and phospho-AKT area ratio ($p<0.0001$, Figure 3.2 B). These findings further support the hypothesis that EGFR plays a critical role in activating the PI3K/AKT signaling pathway in canine STS.

2.4.4. Correlation of PTEN and EGFR expression with clinicopathologic parameters

I examined the correlation between PTEN and EGFR expression with STS types and tumor grades, as illustrated in Figure 3. No significant differences in PTEN expression were observed among different STS types (p=0.910, Figure 3.3 A).

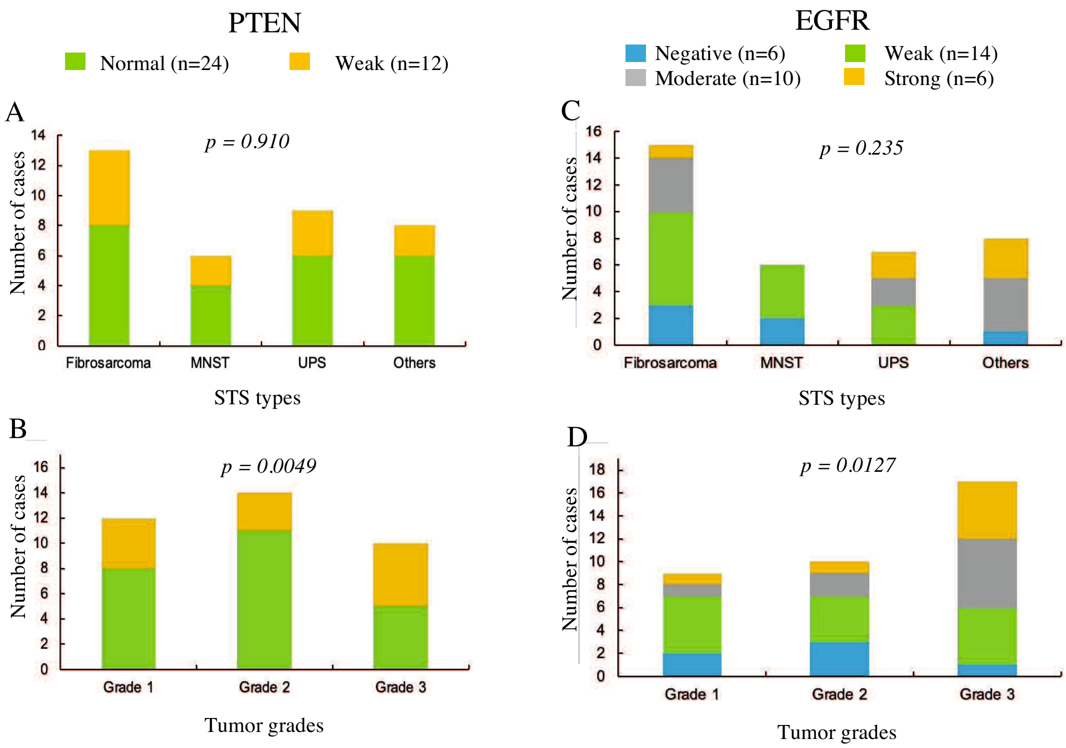

Figure 3.3. *Comparison of EGFR and PTEN expression score among different STS types and grades. There was no statistically significant difference in PTEN and EGFR expression according to STS type (p=0.910 and p=0.235, Figure A and C, respectively). The percentage of PTEN weak expression was found more frequently in samples with high-grade tumors (p=0.0049, B). The percentage of EGFR strong expression was also more frequently found in high-grade tumors (p=0.0127, D). MNST: malignant nerve sheath tumor; UPS: undifferentiated pleomorphic sarcoma.*

Similarly, analysis of EGFR expression revealed no significant differences across STS types (*p*=0.235, Figure 3.3 C). When comparing PTEN expression with tumor grades, weak PTEN expression was notably more frequent in grade 3 STS compared to grades 1 and 2 (*p*=0.0049, Figure 3.3 B). Significant differences in EGFR expression were observed across different tumor grades (*p*=0.0127, Figure 3.3 D).

Finally, I performed multivariate analyses to investigate the correlation between PTEN, EGFR, and *PIK3CA* mutations in conjunction with various clinical and pathological parameters (Figure 3.4). These multivariate analyses revealed that EGFR expression correlated with phospho-AKT level (correlation coefficients 0.68). Furthermore, this analysis did not find any correlation of EGFR and PTEN with other parameters.

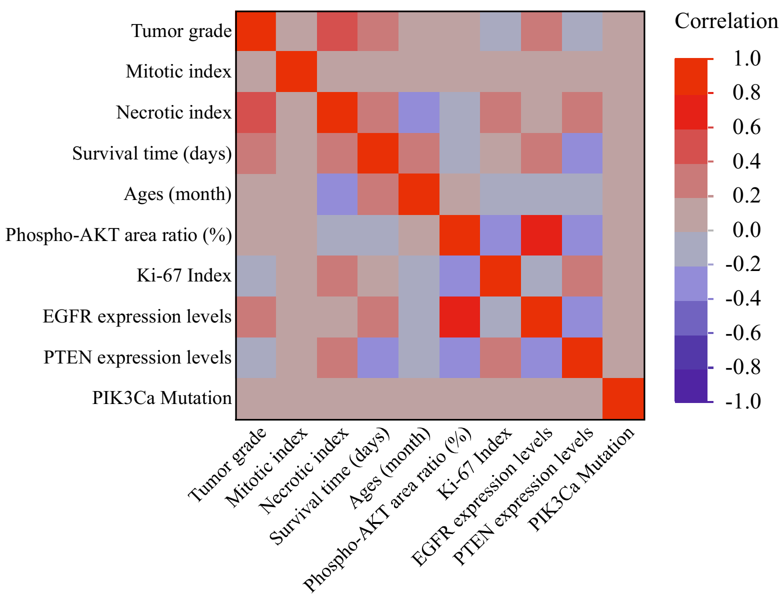

Figure 3.4. *Multivariate analyses indicate that EGFR expression positively correlates to the phospho-AKT area ratio (correlation coefficient, r=0.68).*

2.5 Discussion

Investigating each component of the PI3K/AKT signaling pathway is crucial for elucidating the tumorigenesis mechanism because this pathway plays a pivotal role in regulating many cellular processes (Hoxhaj and Manning 2020). Therefore, several potential factors identified in prior canine studies that might lead to dysregulation of PI3K/AKT signaling pathways were examined. These factors include the loss of PTEN, *PIK3CA mutation*, and EGFR over-expression. By comprehending each component's distinct contributions and interactions, this study potentially offers valuable insights that could aid in identifying biomarkers for early detection and uncovering novel therapeutic targets (Tewari *et al*., 2022).

Similar to human counterparts, *PTEN* mutations or deletions in dogs result in aberrations in the PI3K/AKT signaling pathway, contributing to tumorigenesis (Bazzichetto *et al.*, 2019; Lin *et al.*, 2021). Previous studies in canine hemangiosarcoma (HSA) (Megquier *et al*., 2019), osteosarcoma (OS) (Sarver *et al.*, 2023), and canine mammary tumor (CMT) (Asproni *et al.*, 2021) showed that these malignancies frequently exhibit PTEN loss or reduced expression. PTEN loss was not detected in this investigation. Out of 36 samples, 12 (33.3%) had weak PTEN expression, whereas the remaining had normal expression. The expression of PTEN in samples does not necessarily ensure that these tumor suppressor genes function correctly (Bazzichetto *et al.*, 2019). Therefore, this result does not definitively eliminate the possibility of PTEN interference as a factor contributing to the dysregulation of PI3K/AKT.

One study in human cancer reported that the consecutive activation of the PI3K/AKT signaling pathway is independent of PTEN status in sarcoma cell lines (Lim *et al.*, 2016). In support of the human medicine results, this study indicates the possibility of PTEN-independent and different tumorigenesis mechanisms in canine STS (Mundhenk *et* *al.*, 2011). PTEN independence refers to mechanisms that lead to the activation of the PI3K/AKT pathway without alterations in the *PTEN* gene (Mundhenk *et al.*, 2011). I hypothesize that consecutive PI3K/AKT pathway activation may be caused by other aberrations besides PTEN loss, such as mutations, phosphorylation by tyrosine or serine/threonine kinases, or crosstalk with different pathways.

Furthermore, mutations in the *PIK3CA gene* that can drive the dysregulation of the PI3K/AKT pathway were investigated. *PIK3CA* mutations PIK3CA mutations have been observed in canine HSA (Megquier *et al*., 2019; Estabrooks *et al*., 2023), OS (Choy *et al.*, 2012; Selvarajah *et al.*, 2012), and CMT (Arendt *et al*. 2023; Lee *et al*. 2019). Hotspot mutations such as E545K (located in exon 10) and H1047R (located in exon 21) have been identified in canine cancers, paralleling those observed in human malignancies (Arendt *et al.* 2023; Lee *et al*., 2019). Exon 10 and exon 21 mutations were identified based on DNA sequencing in one sample each.

The prevalence of *PIK3CA* mutations was 12.5%, which is lower than prior investigations conducted on other canine cancers. Previous studies in different types of canine cancers have reported a frequency of *PIK3CA* mutations ranging from 14 – 48% (Arendt *et al*., 2023; Cho *et al*., 2021; Lee *et al*., 2019; Megquier *et al*., 2019; Wang *et al*., 2017). This discrepancy in prevalence might be attributed to the limited number of samples analyzed. The mutation rate in human STS, which is reported at 2.49%, is also notably lower compared to the mutation rates observed in other human cancers, such as breast cancer (36.0%), colorectal cancer (17.9%), and lung carcinoma (9.38%) (Pugh *et al.*, 2022).

The presence of a mutation In *EGFR* leads to continuous activation of downstream signaling pathways, such as the PI3K/AKT pathway, the RAS/RAF/MEK/ERK, and the JAK/STAT pathway (Estabrooks *et al*., 2023). This investigation detected that one out of 12 samples (8.3%) had an *EGFR* mutation in exon 21. It is acknowledged that the lack of mutations does not always indicate that the genes have not been altered. The literature on *EGFR* and other RTK mutations in canine cancer remains sparse. *EGFR* mutations have been reported exclusively in canine adenocarcinoma, albeit with limited prevalence data (Cho *et al.*, 2021; Kobayashi *et al.*, 2023). The mutation analysis of *PIK3CA* and *EGFR* in this study offers additional insights into the genetic alterations associated with canine cancer and aberrant PI3K/AKT signaling pathways.

Using immunolabeling, I identified a direct correlation between EGFR expression and PI3K/AKT signaling activation, as indicated by phospho-AKT expression. Samples with high levels of EGFR expression, indicating potential over-expression, exhibited elevated phospho-AKT area ratio compared to other groups. While the precise mechanism by which EGFR influences PI3K/AKT activation remains unclear, the limited number of mutations detected does not exclude the possibility of EGFR serving as an upstream regulator that triggers the PI3K/AKT dysregulation in canine STS. EGFR over-expression may be attributed to other processes, such as increased transcription, loss of inhibitory signals, defective protein recycling, and gene amplification (Freudlsperger *et al*., 2011; Gaber *et al*., 2014; Guerra *et al*., 2021). EGFR over-expression, which promotes cellular proliferation and the epithelial-mesenchymal transition (EMT), is essential for tumorigenesis and metastasis (McConkey *et al.*, 2009).

The potential utility of PTEN and EGFR as prognostic indicators were analyzed by comparing them with clinicopathological parameters, such as STS subtype and tumor grade. These findings indicated that PTEN's weak expression was significantly associated with tumor grade (p=0.0049). Tumors classified as high-grade (grade 3) STS tend to have weak PTEN expression levels. Moreover, strong EGFR expression levels were significantly associated with high-grade tumors (p=0.0127).

Multivariate analysis also revealed a positive correlation between EGFR and phospho-AKT. A positive correlation score suggests that there may be a greater likelihood of PI3K/AKT activation in canine STS with higher levels of EGFR expression. Phospho-AKT is widely considered a direct marker and primary indicator of the PI3K/AKT signaling pathway activation. A positive correlation between EGFR expression and phospho-AKT indicates that EGFR is likely driving the activation of the PI3K/AKT pathway. This relationship highlights the importance of EGFR and PI3K/AKT signaling in canine STS progression and may inform targeted therapeutic strategies in the future.

GENERAL DISCUSSION

GENERAL DISCUSSION

The first chapter examined canine STS's tumor-infiltrating lymphocytes (TILs) profile. Most STS samples contained intra-tumoral TILs, with CD3+ T cells and CD8+ T cells being the most abundant, while CD20+ B cells and FOXP3+ T-regulatory cells were comparatively limited. This TILs profile indicates that the immune response in STS remains favorable against cancer, as CD3+ and CD8+ T cells subsets are critical for cytotoxic responses against cancer. This study provides novel insights into the role of PI3K/AKT pathway activation in canine STS. A positive correlation between CD8+ T cell density and PI3K/AKT activation was identified, suggesting that this signaling pathway may modulate immune cell infiltration. Furthermore, this investigation identified a correlation between TIL density and the Ki-67 index, a tumor proliferation marker.

Although this study observed correlations between PI3K/AKT activation and TILs density, the directionality and causality of this relationship remain unclear. This positive correlation is suspected to be complex and context-dependent. A plausible mechanism is that elevated PI3K/AKT pathway activity in cancer cells indirectly enhanced tumor-antigen presentation. Activation of the PI3K/AKT pathway increases metabolic activity and upregulates specific proteins, thereby generating stronger immunogenic signals that recruit more TILs to the tumor site. In this context, the relationship may reflect an active immune response as a consequence of the presence of a highly proliferative tumor, as indicated by the association with Ki-67.

Another possibility could be related to the effect of the PI3K/AKT pathway activation to promote the production and secretion of chemokine molecules. Cancer cells' release of these chemokines serves as a chemotactic signal to attract immune cells to the tumor site (Singh and Gray, 2021). Chemokines such as CXCL9 and CXCL10 are reported to attract cytotoxic T lymphocytes (CTLs) by binding to its receptors like CXCR3 (So and

Fruman, 2012), which highly express on CD8+ T cells. The correlation between TILs and PI3K/AKT pathway activation also supports the hypothesis that immune cell infiltration is not simply a passive occurrence but may be actively influenced by tumor proliferation signals.

Similar to findings in human STS, this current study found that canine STS profiles tended to have a low immunosuppressive TME (Chalmers *et al.*, 2017). On the contrary, this investigation found that CD8+ T cells were abundant. However, while CD8+ T cells are often linked to favorable prognosis in several cancers (Khoury *et al.*, 2018; Brummel *et al.*, 2023), the role of TILs as a prognostic marker in current study study remains unclear. The unavailability of complete medical record information limited the ability to analyze CD8+ density as a prognostic indicator.

The first chapter suggests that the PI3K/AKT signaling pathway might not only serve as a prognostic marker for tumor growth and proliferation (Miyanishi *et al.*, 2023) but also play a role in modulating the immune landscape. The positive correlation between CD8+ T cells and the PI3K/AKT pathway may have implications for immunotherapeutic strategies targeting this pathway. This approach could potentially enhance the antitumor immune response. Additionally, the relationship between TILs density and Ki-67 supports the theory that tumor proliferation might drive immune infiltration, highlighting the potential for immune-modulating therapies in conjunction with conventional treatments.

These findings present opportunities for further investigation into the therapeutic targeting of PI3K/AKT to improve treatment outcomes for STS. Previous studies on canine cancers have shown variable levels of TILs. This research provides new insight by directly correlating these immune cells with key oncogenic signaling pathways, such as PI3K/AKT. Detailed analysis of other immune populations, such as macrophages and dendritic cells, which may also influence tumor immune responses, would further enhance the findings of this study. Nevertheless, this study contributes to the existing literature by demonstrating that the presence of CD8+ T cells correlates with PI3K/AKT pathway activation. This suggests a complex relationship between immune infiltration and tumor signaling pathways.

In the second chapter, this study investigates the underlying mechanisms causing PI3K/AKT dysregulation, which may contribute to tumorigenesis. Current study suggests that EGFR over-expression, rather than PTEN loss and PIK3CA mutations, is likely a primary driver of pathway dysregulation. While PTEN loss is one of the common mechanisms for PI3K/AKT dysregulation, no evidence of PTEN loss in canine STS samples. The presence of mutation in only one sample but no hotspot mutations was detected, suggests that PIK3CA alteration might not be a primary driver of this dysregulation. Notably, a significant correlation between high EGFR expression and phospho-AKT levels. This correlation suggests that EGFR over-expression could be a significant factor driving PI3K/AKT pathway dysregulation.

In this study, PI3K/AKT dysregulation was observed to be independent of PTEN status. Loss of PTEN function through mutations or deletions is a well-established mechanism driving tumorigenesis in various human cancers. However, this investigation demonstrated that PTEN was expressed across all samples, with most exhibiting normal expression levels. This observation highlights a potential species-specific mechanism in canine STS. Furthermore, Lim *et al.* (2016) reported, based on an in vitro study using four different human sarcoma cell lines, that PI3K/AKT signaling activation occurred independently of PTEN status, despite normal PTEN protein expression. This indicates that a distinct molecular profile for both human and canine STS differs from other cancers where PTEN loss plays a predominant role.

While PIK3CA gene mutations were detected through DNA sequencing, their low prevalence suggests these mutations are unlikely to be the primary drivers of pathway dysregulation. Only one sample exhibited mutations in exon 10 and exon 21. However, none were located at codons commonly recognized as hotspots mutation (E545K and H1047R) in the PIK3CA gene. This prevalence is considerably lower than previous studies on other canine cancers, where PIK3CA mutation frequencies have ranged from 14% to 48% (Arendt *et al*., 2023; Lee *et al*., 2019; Megquier *et al*., 2019; Moon *et al*., 2016).

A significant finding was the strong correlation between high EGFR expression and elevated phospho-AKT levels. EGFR was expressed in 83.3% of the samples, and most cases (90% of EGFR-positive samples), phospho-AKT levels were also elevated. This result suggests that EGFR over-expression significantly contributes to the PI3K/AKT pathway dysregulation. When EGFR is over-expressed, it facilitates consecutive activation of the downstream PI3K/AKT signaling pathway. This excessive stimulation of EGFR results in cellular change and disrupts the normal regulation of cell growth, survival, and metabolism. The over-expression of EGFR indicates it amplifies the normal processes, contributing to uncontrolled tumor growth and metastasis (Dobashi *et al*., 2009; Moon *et al*., 2016).

EGFR is a cell surface receptor activated by its ligands (such as EGF and TGF-α). This activation initiates a cascade of intracellular signaling pathways. EGFR overexpression increases the number of receptors on the cell surface (Freudlsperger *et al*., 2011). With EGFR overexpression, even normal ligand levels can produce an exaggerated response (Gaber *et al*., 2014). Overexpressed EGFR can undergo ligand-independent activation, where the receptor dimerizes or forms complexes with other receptors (such as HER2 or HER3) even without a ligand (Dobashi *et al*., 2009). All these mechanisms can contribute to consecutive activation of the PI3K/AKT pathway leading to tumorigenesis.

The disruptions of the PI3K/AKT pathway bypass normal cellular checks and balances, allowing for continuous survival and growth of cancer cells (Porta, Paglino and Mosca, 2014; Hoxhaj and Manning, 2020; Meuten *et al*., 2024). This dysregulation not only facilitates the formation of primary tumors but also supports the development of resistance to conventional therapies (Nitulescu *et al*., 2018; Tewari *et al*., 2022; Yu, Wei and Liu, 2022). Additionally, the interplay between EGFR over-expression and PI3K/AKT activation may contribute to the tumor's ability to evade immune surveillance, further complicating treatment strategies.

Given the central role of EGFR in activating the PI3K/AKT pathway, targeting this receptor may provide a promising therapeutic approach (So and Fruman, 2012; LoRusso, 2016; Mayer and Arteaga, 2016). EGFR inhibitors, such as cetuximab or gefitinib, have been explored in human cancer therapy (Freudlsperger *et al*. 2011; Gaber *et al*. 2014), and similar strategies could be repurposed in dogs. Further research into the molecular mechanisms linking EGFR over-expression with PI3K/AKT dysregulation will be crucial in identifying novel treatments to modulate this pathway and improve outcomes for patients with cancers driven by EGFR-mediated signaling.

The limitation of this study was the inability to identify reliable markers for predicting metastasis, recurrence, and overall survival. One of the primary goals of this investigation was to identify markers for distinguishing high-risk cases. However, the retrospective nature of the sample collection and incomplete clinical data posed significant limitations. Not all samples had complete records regarding metastasis status, recurrence, or survival times. The lack of comprehensive clinical data limited the ability to establish correlations between protein expression and prognostic indicators. Future studies with prospectively collected samples and well-documented clinical outcomes are essential to establish the prognostic value of canine STS.

In conclusion, this study highlights EGFR over-expression as a prominent feature and potential driver of PI3K/AKT pathway activation in canine STS, opening up new avenues for targeted therapies in veterinary oncology. These findings underscore the need for additional research to better understand the molecular mechanisms in canine STS and validate potential therapeutic targets.

CONCLUSION

1. TILs density was positively correlated with the activation of the PI3K/AKT signaling pathway. The group with high levels of phospho-AKT and phospho-S6 tended to have a higher CD8+ T cells density. A higher proliferation rate, as suggested by a high Ki-67 index, indicates a higher number of CD3+, CD8+, and CD20+ TILs.
2. The aberrant PI3K/AKT signaling pathway in canine STS may be related to the high expression of EGFR. The absence of PTEN loss and low PIK3CA mutation prevalence indicate that both are unlikely the main contributors to PI3K/AKT dysregulation in canine STS.

ACKNOWLEDGEMENT

I sincerely express my deepest gratitude to the distinguished individuals and institutions whose invaluable contributions have been integral to the completion of this doctoral research. This study was conducted at the Laboratory of Molecular Diagnostics and Therapeutics, Joint Graduate School of Veterinary Medicine, Yamaguchi University, Japan, from 2021 to 2025. First and foremost, I express my deepest gratitude to Allah SWT and Prophet Muhammad SAW, whose blessings and guidance have allowed me to reach this milestone in my academic journey.

I am deeply grateful to express my utmost appreciation to my supervisor, Prof. Takuya Mizuno. His exceptional attention, guidance, knowledge, and unwavering support have been instrumental throughout my doctoral study. I sincerely appreciate the opportunity to work under his guidance. Studying under his mentorship has been an invaluable learning experience that has profoundly shaped my growth during this study.

My heartfelt gratitude also extends to my co-supervisor and graduate committee members, Prof. Masaru Okuda, Assoc.Prof. Kenji Baba, Prof. Yasuyuki Endo, Prof. Masahiro Morimoto, and Prof. Kenji Tani, for their insightful feedback and suggestions, which have significantly enhanced the quality of this research. Special thanks to Dr. Masaya Igase, Dr. Satoshi Kambayashi, and Dr. Shoma Nishibori for their encouragement, thoughtful discussions, motivation, and generous guidance throughout my studies. I am also profoundly grateful to the Yamaguchi University Animal Medical Center staff for allowing me to participate in clinical practice during my study.

This study was made possible by the generous financial support of the Japan's Ministry of Education, Culture, Sports, Science, and Technology (Monbukagakusho). I sincerely thank the Joint Graduate School of Veterinary Medicine, Yamaguchi University and Faculty of Veterinary Medicine, Gadjah Mada University (UGM), for making this doctoral study possible. I also extend my profound gratitude to all the staff in the Department of Internal Medicine, Faculty of Veterinary Medicine, UGM, for their unwavering support throughout my academic journey.

I also thank all Laboratory of Molecular Diagnostics and Therapeutics members for their guidance, collaboration, and willingness to share knowledge. I also thank Ms. Kumi Inoue and Mizue Sumita for their technical assistance with the experiment. I also extend my gratitude to everyone who, directly or indirectly, has contributed to the success of this dissertation. This accomplishment would not have been possible without the kindness, assistance, and encouragement of these individuals and organizations.

Finally, my heartfelt thanks go to my family, whose love, prayers, and encouragement have been my greatest source of strength. My deepest grateful are extended to my wife, Dhasia Ramandani, thank you for your unwavering support and countless sacrifices for my life. I wish to convey my sincere appreciation for your support, encouragement, and prayers throughout this academic pursuit. To my beloved son, Raffasya Ziyad Athaya, you have been my greatest motivation throughout this journey. I am also deeply indebted to my parents, Saimun and Muntiyanah, and my parents-in-law, Yudo Prasetyo and Kusiah, and all family members for their unconditional love, prayers, and support. Thank you.

REFERENCES

Abrams, B. E., Putterman, A. B., Ruple, A., Wavreille, V., & Selmic, L. E. (2021). Variability in tumor margin reporting for soft tissue sarcoma and cutaneous mast cell tumors in dogs: A systematic review. Veterinary Surgery, 50(2), 259–272. https://doi.org/10.1111/vsu.13539

Adams, V. J., Evans, K. M., Sampson, J., & Wood, J. L. N. (2010). Methods and mortality results of a health survey of purebred dogs in the UK. Journal of Small Animal Practice, 51(10), 512–524. https://doi.org/10.1111/j.1748-5827.2010.00974.x

Alliouachene, S., Tuttle, R. L., Boumard, S., Lapointe, T., Berissi, S., Germain, S., Jaubert, F., Tosh, D., Birnbaum, M. J., & Pende, M. (2008). Constitutively active Akt1 expression in mouse pancreas requires S6 kinase 1 for insulinoma formation. Journal of Clinical Investigation, 118(11), 3629–3638. https://doi.org/10.1172/JCI35237

Amin, M. A., Haas, C. S., Zhu, K., Mansfield, P. J., Kim, M. J., Lackowski, N. P., & Koch, A. E. (2006). Migration inhibitory factor up-regulates vascular cell adhesion molecule-1 and intercellular adhesion molecule-1 via Src, PI3 kinase, and NFκB. Blood, 107(6), 2252–2261. https://doi.org/10.1182/blood-2005-05-2011

Arendt, M. L., Sakthikumar, S., Melin, M., Elvers, I., Rivera, P., Larsen, M., Saellström, S., Lingaas, F., Rönnberg, H., & Lindblad-Toh, K. (2023a). PIK3CA is recurrently mutated in canine mammary tumors, similarly to in human mammary neoplasia. Scientific Reports, 13(1). https://doi.org/10.1038/s41598-023-27664-7

Argyle, D., & Khanna, C. (2020). The Biology of Cancer: in Withrow and MacEwen's Small Animal Clinical Oncology (S. Withrow & D. Vail, Eds.). Elsevier. https://doi.org/10.1016/C2016-0-01939-3

Asproni, P., Millanta, F., Ressel, L., Podestà, F., Parisi, F., Vannozzi, I., & Poli, A. (2021). An immunohistochemical study of the pten/akt pathway involvement in canine and feline mammary tumors. Animals, 11(2), 1–15. https://doi.org/10.3390/ani11020365

Badalamenti, G., Fanale, D., Incorvaia, L., Barraco, N., Listì, A., Maragliano, R., Vincenzi, B., Calò, V., Iovanna, J. L., Bazan, V., & Russo, A. (2019). Role of tumor-infiltrating lymphocytes in patients with solid tumors: Can a drop dig a stone? Cellular Immunology, 343, 103753. https://doi.org/10.1016/j.cellimm.2018.01.013

Baioni, E., Scanziani, E., Vincenti, M. C., Leschiera, M., Bozzetta, E., Pezzolato, M., Desiato, R., Bertolini, S., Maurella, C., & Ru, G. (2017). Estimating canine cancer incidence: Findings from a population-based tumour registry in northwestern Italy. BMC Veterinary Research, 13(1). https://doi.org/10.1186/s12917-017-1126-0

Bazzichetto, C., Conciatori, F., Pallocca, M., Falcone, I., Fanciulli, M., Cognetti, F., Milella, M., & Ciuffreda, L. (2019). Pten as a prognostic/predictive biomarker in cancer: An unfulfilled promise? Cancers, 11(4). https://doi.org/10.3390/cancers11040435

Bray, J. P. (2016). Soft tissue sarcoma in the dog - part 1: a current review. Journal of Small Animal Practice, 57(10), 510–519. https://doi.org/10.1111/jsap.12556

Bray, J. P. (2017). Soft tissue sarcoma in the dog – Part 2: surgical margins, controversies and a comparative review. In Journal of Small Animal Practice (Vol. 58, Issue 2, pp. 63–72). Blackwell Publishing Ltd. https://doi.org/10.1111/jsap.12629

Brummel, K., Eerkens, A. L., de Bruyn, M., & Nijman, H. W. (2023). Tumour-infiltrating lymphocytes: from prognosis to treatment selection. In British Journal of Cancer (Vol. 128, Issue 3, pp. 451–458). Springer Nature. https://doi.org/10.1038/s41416-022-02119-4

Bujak, J. K., Szopa, I. M., Pingwara, R., Kruczyk, O., Krzemińska, N., Mucha, J., & Majchrzak-Kuligowska, K. (2020). The Expression of Selected Factors Related to T Lymphocyte Activity in Canine Mammary Tumors. International Journal of Molecular Sciences, 21(7). https://doi.org/10.3390/ijms21072292

Burton, J. H., Mitchell, L., Thamm, D. H., Dow, S. W., & Biller, B. J. (2011). Low-Dose Cyclophosphamide Selectively Decreases Regulatory T Cells and Inhibits Angiogenesis in Dogs with Soft Tissue Sarcoma. Journal of Veterinary Internal Medicine, 25(4), 920–926. https://doi.org/10.1111/j.1939-1676.2011.0753.x

Campos, M., Kool, M. M. J., Daminet, S., Ducatelle, R., Rutteman, G., Kooistra, H. S., Galac, S., & Mol, J. A. (2014). Upregulation of the PI3K/Akt Pathway in the Tumorigenesis of Canine Thyroid Carcinoma. Journal of Veterinary Internal Medicine, 28(6), 1814–1823. https://doi.org/10.1111/jvim.12435

Carvalho, M. I., Pires, I., Prada, J., & Queiroga, F. L. (2011). T-lymphocytic infiltrate in canine mammary tumours: clinic and prognostic implications. In Vivo (Athens, Greece), 25(6), 963–969.

Chalmers, Z. R., Connelly, C. F., Fabrizio, D., Gay, L., Ali, S. M., Ennis, R., Schrock, A., Campbell, B., Shlien, A., Chmielecki, J., Huang, F., He, Y., Sun, J., Tabori, U., Kennedy, M., Lieber, D. S., Roels, S., White, J., Otto, G. A., … Frampton, G. M. (2017). Analysis of 100,000 human cancer genomes reveals the landscape of tumor mutational burden. Genome Medicine, 9(1), 34. https://doi.org/10.1186/s13073-017-0424-2

Chiti, L. E., Ferrari, R., Boracchi, P., Morello, E., Marconato, L., Roccabianca, P., Avallone, G., Iussich, S., Giordano, A., Ferraris, E. I., Agnoli, C., Dondi, F., Giacobino, D., Godizzi, F., & Stefanello, D. (2021). Prognostic impact of clinical, haematological, and histopathological variables in 102 canine cutaneous perivascular wall tumours. Veterinary and Comparative Oncology, 19(2), 275–283. https://doi.org/10.1111/vco.12673

Cho, S. H., Seung, B. J., Kim, S. H., Bae, M. K., Lim, H. Y., & Sur, J. H. (2021). EGFR Overexpression and Sequence Analysis of KRAS, BRAF, and EGFR Mutation Hot Spots in Canine Intestinal Adenocarcinoma. Veterinary Pathology, 58(4), 674–682. https://doi.org/10.1177/03009858211009778

Choy, E., Hornicek, F., MacConaill, L., Harmon, D., Tariq, Z., Garraway, L., & Duan, Z. (2012). High-throughput genotyping in osteosarcoma identifies multiple mutations in phosphoinositide-3-kinase and other oncogenes. Cancer, 118(11), 2905–2914. https://doi.org/10.1002/cncr.26617

Coindre, J. (2006). Grading of Soft Tissue Sarcomas Review and Update. In Arch Pathol Lab Med (Vol. 130).

Dell'Anno, F., Giugliano, R., Listorti, V., & Razzuoli, E. (2024). A Review on Canine and Human Soft Tissue Sarcomas: New Insights on Prognosis Factors and Treatment

Measures. In Veterinary Sciences (Vol. 11, Issue 8). Multidisciplinary Digital Publishing Institute (MDPI). https://doi.org/10.3390/vetsci11080362

Dennis, M. M., McSporran, K. D., Bacon, N. J., Schulman, F. Y., Foster, R. A., & Powers, B. E. (2011). Prognostic Factors for Cutaneous and Subcutaneous Soft Tissue Sarcomas in Dogs. Veterinary Pathology, 48(1), 73–84. https://doi.org/10.1177/0300985810388820

Dhein, E. S., Heikkilä, U., Oevermann, A., Blatter, S., Meier, D., Hartnack, S., & Guscetti, F. (2024). Incidence rates of the most common canine tumors based on data from the Swiss Canine Cancer Registry (2008 to 2020). PLoS ONE, 19(4 April). https://doi.org/10.1371/journal.pone.0302231

Dobashi, Y., Suzuki, S., Sato, E., Hamada, Y., Yanagawa, T., & Ooi, A. (2009a). EGFR-dependent and independent activation of Akt/mTOR cascade in bone and soft tissue tumors. Modern Pathology, 22(10), 1328–1340. https://doi.org/10.1038/modpathol.2009.104

Dobromylskyj, M. (2022). Feline Soft Tissue Sarcomas: A Review of the Classification and Histological Grading, with Comparison to Human and Canine. In Animals (Vol. 12, Issue 20). MDPI. https://doi.org/10.3390/ani12202736

Estabrooks, T., Gurinovich, A., Pietruska, J., Lewis, B., Harvey, G., Post, G., Lambert, L., Miller, A., Rodrigues, L., White, M. E., Lopes, C., London, C. A., & Megquier, K. (2023). Identification of genomic alterations with clinical impact in canine splenic hemangiosarcoma. Veterinary and Comparative Oncology, 21(4), 623–633. https://doi.org/10.1111/vco.12925

Freudlsperger, C., Burnett, J. R., Friedman, J. A., Kannabiran, V. R., Chen, Z., & Van Waes, C. (2011). EGFR-PI3K-AKT-mTOR signaling in head and neck squamous cell carcinomas: Attractive targets for molecular-oriented therapy. In Expert Opinion on Therapeutic Targets (Vol. 15, Issue 1, pp. 63–74). https://doi.org/10.1517/14728222.2011.541440

Gaber, R., Watermann, I., Kugler, C., Reinmuth, N., Huber, R. M., Schnabel, P. A., Vollmer, E., Reck, M., & Goldmann, T. (2014). Correlation of EGFR expression, gene copy number and clinicopathological status in NSCLC. http://www.diagnosticpathology.org/content/9/1/165

Gardner, H. L., Fenger, J. M., London, C. A., & Heatre, G. (2016). Dogs as a model for cancer. In Annual Review of Animal Biosciences (Vol. 4, pp. 199–222). Annual Reviews Inc. https://doi.org/10.1146/annurev-animal-022114-110911

Gori, S., Sidoni, A., Colozza, M., Ferri, I., Mameli, M. G., Fenocchio, D., Stocchi, L., Foglietta, J., Ludovini, V., Minenza, E., De Angelis, V., & Crinò, L. (2009). EGFR, pMAPK, pAkt and PTEN status by immunohistochemistry: Correlation with clinical outcome in HER2-positive metastatic breast cancer patients treated with trastuzumab. Annals of Oncology, 20(4), 648–654. https://doi.org/10.1093/annonc/mdn681

Greten, F. R., & Grivennikov, S. I. (2019). Inflammation and Cancer: Triggers, Mechanisms, and Consequences. Immunity, 51(1), 27–41. https://doi.org/10.1016/j.immuni.2019.06.025

Guerra, F., Quintana, S., Giustina, S., Mendeluk, G., Jufe, L., Avagnina, M. A., Díaz, L. B., & Palaoro, L. A. (2021). Investigation of EGFR/pi3k/Akt signaling pathway in seminomas. Biotechnic and Histochemistry, 96(2), 125–137. https://doi.org/10.1080/10520295.2020.1776393

Hawkins, P. T., & Stephens, L. R. (2015). PI3K signalling in inflammation. Biochimica et Biophysica Acta (BBA) - Molecular and Cell Biology of Lipids, 1851(6), 882–897. https://doi.org/10.1016/j.bbalip.2014.12.006

Haydinger, C. D., Ashander, L. M., Tan, A. C. R., & Smith, J. R. (2023). Intercellular Adhesion Molecule 1: More than a Leukocyte Adhesion Molecule. Biology, 12(5), 743. https://doi.org/10.3390/biology12050743

He, Y., Sun, M. M., Zhang, G. G., Yang, J., Chen, K. S., Xu, W. W., & Li, B. (2021). Targeting PI3K/Akt signal transduction for cancer therapy. In Signal Transduction and Targeted Therapy (Vol. 6, Issue 1). Springer Nature. https://doi.org/10.1038/s41392-021-00828-5

Hoxhaj, G., & Manning, B. D. (2020). The PI3K–AKT network at the interface of oncogenic signalling and cancer metabolism. In Nature Reviews Cancer (Vol. 20, Issue 2, pp. 74–88). Nature Research. https://doi.org/10.1038/s41568-019-0216-7

Hsieh, A. C., Costa, M., Zollo, O., Davis, C., Feldman, M. E., Testa, J. R., Meyuhas, O., Shokat, K. M., & Ruggero, D. (2010). Genetic Dissection of the Oncogenic mTOR Pathway Reveals Druggable Addiction to Translational Control via 4EBP-eIF4E. Cancer Cell, 17(3), 249–261. https://doi.org/10.1016/j.ccr.2010.01.021

Judge, S. J., Bloomstein, J. D., Sholevar, C. J., Darrow, M. A., Stoffel, K. M., Vick, L. V., Dunai, C., Cruz, S. M., Razmara, A. M., Monjazeb, A. M., Rebhun, R. B., Murphy, W. J., & Canter, R. J. (2022). Transcriptome Analysis of Tumor-Infiltrating Lymphocytes Identifies NK Cell Gene Signatures Associated With Lymphocyte Infiltration and Survival in Soft Tissue Sarcomas. Frontiers in Immunology, 13. https://doi.org/10.3389/fimmu.2022.893177

Khoury, T., Nagrale, V., Opyrchal, M., Peng, X., Wang, D., & Yao, S. (2018). Prognostic Significance of Stromal Versus Intratumoral Infiltrating Lymphocytes in Different Subtypes of Breast Cancer Treated With Cytotoxic Neoadjuvant Chemotherapy. Applied Immunohistochemistry & Molecular Morphology, 26(8), 523–532. https://doi.org/10.1097/PAI.0000000000000466

Kim, S. H., Seung, B. J., Cho, S. H., Lim, H. Y., Bae, M. K., & Sur, J. H. (2021). Dysregulation of pi3k/akt/pten pathway in canine mammary tumor. Animals, 11(7). https://doi.org/10.3390/ani11072079

Kobayashi, K., Takemura, R. D., Miyamae, J., Mitsui, I., Murakami, K., Kutara, K., Saeki, K., Kanda, T., Okamura, Y., & Sugiyama, A. (2023). Phenotypic and molecular characterization of novel pulmonary adenocarcinoma cell lines established from a dog. Scientific Reports, 13(1), 16823. https://doi.org/10.1038/s41598-023-44062-1

Kong, D.-H., Kim, Y., Kim, M., Jang, J., & Lee, S. (2018). Emerging Roles of Vascular Cell Adhesion Molecule-1 (VCAM-1) in Immunological Disorders and Cancer. International Journal of Molecular Sciences, 19(4), 1057. https://doi.org/10.3390/ijms19041057

Kuntz, C. A., Dernell, W. S., Powers, B. E., Devitt, C., Straw, R. C., & Withrow, S. J. (1997). Prognostic factors for surgical treatment of soft-tissue sarcomas in dogs: 75 cases (1986-1996). Journal of the American Veterinary Medical Association, 211(9), 1147–1151.

Lee, K. H., Hwang, H. J., Noh, H. J., Shin, T. J., & Cho, J. Y. (2019). Somatic mutation of PIK3ca (H1047R) is a common driver mutation hotspot in canine mammary tumors as well as human breast cancers. Cancers, 11(12). https://doi.org/10.3390/cancers11122006

Lenz, J. A., Assenmacher, C.-A., Costa, V., Louka, K., Rau, S., Keuler, N. S., Zhang, P. J., Maki, R. G., Durham, A. C., Radaelli, E., & Atherton, M. J. (2022). Increased tumor-infiltrating lymphocyte density is associated with favorable outcomes in a comparative study of canine histiocytic sarcoma. Cancer Immunology, Immunotherapy, 71(4), 807–818. https://doi.org/10.1007/s00262-021-03033-z

Li, L. T., Jiang, G., Chen, Q., & Zheng, J. N. (2015). Predic Ki67 is a promising molecular target in the diagnosis of cancer (Review). In Molecular Medicine Reports (Vol. 11, Issue 3, pp. 1566–1572). Spandidos Publications. https://doi.org/10.3892/mmr.2014.2914

Lim, H. J., Wang, X., Crowe, P., Goldstein, D., & Yang, J. L. (2016). Targeting the PI3K/PTEN/AKT/mTOR pathway in treatment of sarcoma cell lines. Anticancer Research, 36(11), 5765–5771. https://doi.org/10.21873/anticanres.11160

Lin, Z., Huang, L., Li, S. L., Gu, J., Cui, X., & Zhou, Y. (2021). PTEN loss correlates with T cell exclusion across human cancers. BMC Cancer, 21(1). https://doi.org/10.1186/s12885-021-08114-x

Liptak, J. M., & Forrest, L. J. (2013). Withrow & MacEwen's Small Animal Clinical Oncology (Vol. 5th).

Loi, S., Michiels, S., Adams, S., Loibl, S., Budczies, J., Denkert, C., & Salgado, R. (2021). The journey of tumor-infiltrating lymphocytes as a biomarker in breast cancer: clinical utility in an era of checkpoint inhibition. Annals of Oncology, 32(10), 1236–1244. https://doi.org/10.1016/j.annonc.2021.07.007

Lorch, G., Sivaprakasam, K., Zismann, V., Perdigones, N., Contente-Cuomo, T., Nazareno, A., Facista, S., Wong, S., Drenner, K., Liang, W. S., Amann, J. M., Sinicropi-Yao, S. L., Koenig, M. J., Perle, K. La, Whitsett, T. G., Murtaza, M., Trent, J. M., Carbone, D. P., & Hendricks, W. P. D. (2019). Identification of recurrent activating HER2 mutations in primary canine pulmonary adenocarcinoma. Clinical Cancer Research, 25(19), 5866–5877. https://doi.org/10.1158/1078-0432.CCR-19-1145

LoRusso, P. M. (2016). Inhibition of the PI3K/AKT/mTOR pathway in solid tumors. Journal of Clinical Oncology, 34(31), 3803–3815. https://doi.org/10.1200/JCO.2014.59.0018

Mafi, S., Mansoori, B., Taeb, S., Sadeghi, H., Abbasi, R., Cho, W. C., & Rostamzadeh, D. (2022). mTOR-Mediated Regulation of Immune Responses in Cancer and Tumor Microenvironment. Frontiers in Immunology, 12. https://doi.org/10.3389/fimmu.2021.774103

Mayer, I. A., & Arteaga, C. L. (2016). The PI3K/AKT pathway as a target for cancer treatment. Annual Review of Medicine, 67, 11–28. https://doi.org/10.1146/annurev-med-062913-051343

McConkey, D. J., Choi, W., Marquis, L., Martin, F., Williams, M. B., Shah, J., Svatek, R., Das, A., Adam, L., Kamat, A., Siefker-Radtke, A., & Dinney, C. (2009). Role of epithelial-to-mesenchymal transition (EMT) in drug sensitivity and metastasis in bladder cancer. Cancer and Metastasis Reviews, 28(3–4), 335–344. https://doi.org/10.1007/s10555-009-9194-7

McSporran, K. D. (2009). Histologic Grade Predicts Recurrence for Marginally Excised Canine Subcutaneous Soft Tissue Sarcomas. Veterinary Pathology, 46(5), 928–933. https://doi.org/10.1354/vp.08-VP-0277-M-FL

Megquier, K., Turner-Maier, J., Swofford, R., Kim, J. H., Sarver, A. L., Wang, C., Sakthikumar, S., Johnson, J., Koltookian, M., Lewellen, M., Scott, M. C., Schulte, A. J., Borst, L., Tonomura, N., Alfoldi, J., Painter, C., Thomas, R., Karlsson, E. K., Breen, M., … Lindblad-Toh, K. (2019). Comparative genomics reveals shared mutational landscape in canine hemangiosarcoma and human angiosarcoma. Molecular Cancer Research, 17(12), 2410–2421. https://doi.org/10.1158/1541-7786.MCR-19-0221

Meuten, T. K., Dean, G. A., & Thamm, D. H. (2024). Review: The PI3K-AKT-mTOR signal transduction pathway in canine cancer. In Veterinary Pathology (Vol. 61, Issue 3, pp. 339–356). SAGE Publications Inc. https://doi.org/10.1177/03009858231207021

Meuten, T. K., Dean, G. A., Thamm, D. H., & Travis, M. (2024). Review: The PI3K-AKT-mTOR signal transduction pathway in canine cancer. In Veterinary Pathology (Vol. 61, Issue 3, pp. 339–356). SAGE Publications Inc. https://doi.org/10.1177/03009858231207021

Misdorp, W. (1976). Histologic classification and further characterization of tumors in domestic animals. Advances in Veterinary Science and Comparative Medicine, 20, 191–221.

Mitchell, K. G., Parra, E. R., Nelson, D. B., Zhang, J., Wistuba, I. I., Fujimoto, J., Roth, J. A., Antonoff, M. B., Corsini, E. M., Vaporciyan, A. A., Hofstetter, W. L., Mehran, R. J., Swisher, S. G., Rice, D. C., Sepesi, B., Walsh, G. L., Behrens, C., Kalhor, N., Weissferdt, A., … Lee, J. J. (2019). Tumor cellular proliferation is associated with enhanced immune checkpoint expression in stage I non–small cell lung cancer. The Journal of Thoracic and Cardiovascular Surgery, 158(3), 911-919.e6. https://doi.org/10.1016/j.jtcvs.2019.04.084

Miyanishi, K., Nururrozi, A., Igase, M., Tanabe, M., Sakurai, M., Sakai, Y., Shimonohara, N., Murakami, M., & Mizuno, T. (2023). Activation of the Akt signalling pathway as a prognostic indicator in canine soft tissue sarcoma. Journal of Comparative Pathology, 206, 44–52. https://doi.org/10.1016/j.jcpa.2023.08.007

Moon, A., Chin, S., Kim, H. K., Kwak, J. J., Koh, E. S., Kim, Y. W., & Jang, K. T. (2016). EGFR, COX2, p-AKT expression and PIK3CA mutation in distal extrahepatic bile duct carcinoma. Pathology, 48(1), 35–40. https://doi.org/10.1016/j.pathol.2015.11.011

Mundhenk, J., Hennenlotter, J., Zug, L., Alloussi, S. H., Todenhoefer, T., Gakis, G., Aufderklamm, S., Scharpf, M., Kuehs, U., Stenzl, A., & Schwentner, C. (2011). Evidence for PTEN-independent Akt activation and Akt-independent p27Kip1 expression in advanced bladder cancer. Oncology Letters, 2(6), 1089–1093. https://doi.org/10.3892/ol.2011.374

Nitulescu, G. M., Van De Venter, M., Nitulescu, G., Ungurianu, A., Juzenas, P., Peng, Q., Olaru, O. T., Grădinaru, D., Tsatsakis, A., Tsoukalas, D., Spandidos, D. A., & Margina, D. (2018). The Akt pathway in oncology therapy and beyond (Review). In International Journal of Oncology (Vol. 53, Issue 6, pp. 2319–2331). Spandidos Publications. https://doi.org/10.3892/ijo.2018.4597

Nyström, H., Jönsson, M., Nilbert, M., & Carneiro, A. (2023). Immune-cell infiltration in high-grade soft tissue sarcomas; prognostic implications of tumor-associated macrophages and B-cells. Acta Oncologica, 62(1), 33–39. https://doi.org/10.1080/0284186X.2023.2172688

Ocana, A., Vera-Badillo, F., Al-Mubarak, M., Templeton, A. J., Corrales-Sanchez, V., Diez-Gonzalez, L., Cuenca-Lopez, M. D., Seruga, B., Pandiella, A., & Amir, E. (2014). Activation of the PI3K/mTOR/AKT pathway and survival in solid tumors: Systematic review and meta-analysis. PLoS ONE, 9(4). https://doi.org/10.1371/journal.pone.0095219

Perry, J. A., Culp, W. T. N., Dailey, D. D., Eickhoff, J. C., Kamstock, D. A., & Thamm, D. H. (2014). Diagnostic accuracy of pre-treatment biopsy for grading soft tissue sarcomas in dogs. Veterinary and Comparative Oncology, 12(2), 106–113. https://doi.org/10.1111/j.1476-5829.2012.00333.x

Pillozzi, S., Bernini, A., Palchetti, I., Crociani, O., Antonuzzo, L., Campanacci, D., & Scoccianti, G. (2021). Soft tissue sarcoma: An insight on biomarkers at molecular, metabolic and cellular level. In Cancers (Vol. 13, Issue 12). MDPI. https://doi.org/10.3390/cancers13123044

Pinard, C. J., Lagree, A., Lu, F.-I., Klein, J., Oblak, M. L., Salgado, R., Cardenas, J. C. P., Brunetti, B., Muscatello, L. V., Sarli, G., Foschini, M. P., Hardas, A., Castillo, S. P., AbdulJabbar, K., Yuan, Y., Moore, D. A., & Tran, W. T. (2022). Comparative Evaluation of Tumor-Infiltrating Lymphocytes in Companion Animals: Immuno-Oncology as a Relevant Translational Model for Cancer Therapy. Cancers, 14(20), 5008. https://doi.org/10.3390/cancers14205008

Porcellato, I., Silvestri, S., Menchetti, L., Recupero, F., Mechelli, L., Sforna, M., Iussich, S., Bongiovanni, L., Lepri, E., & Brachelente, C. (2020). Tumour-infiltrating lymphocytes in canine melanocytic tumours: An investigation on the prognostic role of CD3 + and CD20 + lymphocytic populations. Veterinary and Comparative Oncology, 18(3), 370–380. https://doi.org/10.1111/vco.12556

Porta, C., Paglino, C., & Mosca, A. (2014). Targeting PI3K/Akt/mTOR signaling in cancer. In Frontiers in Oncology: Vol. 4 APR. Frontiers Research Foundation. https://doi.org/10.3389/fonc.2014.00064

Powell, J. D., Pollizzi, K. N., Heikamp, E. B., & Horton, M. R. (2012). Regulation of Immune Responses by mTOR. Annual Review of Immunology, 30(1), 39–68. https://doi.org/10.1146/annurev-immunol-020711-075024

Presti, D., Dall'Olio, F. G., Besse, B., Ribeiro, J. M., Di Meglio, A., & Soldato, D. (2022). Tumor infiltrating lymphocytes (TILs) as a predictive biomarker of response to checkpoint blockers in solid tumors: A systematic review. In Critical Reviews in Oncology/Hematology (Vol. 177). Elsevier Ireland Ltd. https://doi.org/10.1016/j.critrevonc.2022.103773

Pugh, T. J., Bell, J. L., Bruce, J. P., Doherty, G. J., Galvin, M., Green, M. F., Hunter-Zinck, H., Kumari, P., Lenoue-Newton, M. L., Li, M. M., Lindsay, J., Mazor, T., Ovalle, A., Sammut, S.-J., Schultz, N., Yu, T. V., Sweeney, S. M., & Bernard, B. (2022). AACR Project GENIE: 100,000 Cases and Beyond. Cancer Discovery, 12(9), 2044–2057. https://doi.org/10.1158/2159-8290.CD-21-1547

Quail, D. F., & Joyce, J. A. (2013). Microenvironmental regulation of tumor progression and metastasis. Nature Medicine, 19(11), 1423–1437. https://doi.org/10.1038/nm.3394

Rao, R. R., Li, Q., Odunsi, K., & Shrikant, P. A. (2010). The mTOR Kinase Determines Effector versus Memory CD8 + T Cell Fate by Regulating the Expression of Transcription Factors T-bet and Eomesodermin. Immunity, 32(1), 67–78. https://doi.org/10.1016/j.immuni.2009.10.010

Saeki, K., Endo, Y., Uchida, K., Nishimura, R., Sasaki, N., & Nakagawa, T. (2012). Significance of Tumor-Infiltrating Immune Cells in Spontaneous Canine Mammary Gland Tumor: 140 Cases. Journal of Veterinary Medical Science, 74(2), 227–230. https://doi.org/10.1292/jvms.11-0118

Sakai, K., Maeda, S., Yamada, Y., Chambers, J. K., Uchida, K., Nakayama, H., Yonezawa, T., & Matsuki, N. (2018). Association of tumour-infiltrating regulatory T cells with adverse outcomes in dogs with malignant tumours. Veterinary and Comparative Oncology, 16(3), 330–336. https://doi.org/10.1111/vco.12383

Sakai, O., Ii T, Uchida, K., Igase, M., Mizuno T. (2020). Establishment and characterization of monoclonal antibody against canine CD8 alpha. Monoclon Antib Immunodiagn Immunother 39(4): 129- 134. DOI: 10.1089/mab.2020.0002

Salgado, R., Denkert, C., Demaria, S., Sirtaine, N., Klauschen, F., Pruneri, G., Wienert, S., Van den Eynden, G., Baehner, F. L., Penault-Llorca, F., Perez, E. A., Thompson, E. A., Symmans, W. F., Richardson, A. L., Brock, J., Criscitiello, C., Bailey, H., Ignatiadis, M., Floris, G., … Loi, S. (2015). The evaluation of tumor-infiltrating lymphocytes (TILs) in breast cancer: recommendations by an International TILs Working Group 2014. Annals of Oncology, 26(2), 259–271. https://doi.org/10.1093/annonc/mdu450

Sambri, A., Caldari, E., Fiore, M., Zucchini, R., Giannini, C., Pirini, M. G., Spinnato, P., Cappelli, A., Donati, D. M., & De Paolis, M. (2021). Margin assessment in soft tissue sarcomas: Review of the literature. In Cancers (Vol. 13, Issue 7). MDPI AG. https://doi.org/10.3390/cancers13071687

Sarver, A. L., Makielski, K. M., DePauw, T. A., Schulte, A. J., & Modiano, J. F. (2022). Increased risk of cancer in dogs and humans: A consequence of recent extension of lifespan beyond evolutionarily determined limitations? Aging and Cancer, 3(1), 3–19. https://doi.org/10.1002/aac2.12046

Sarver, A. L., Mills, L. J., Makielski, K. M., Temiz, N. A., Wang, J., Spector, L. G., Subramanian, S., & Modiano, J. F. (2023). Distinct mechanisms of PTEN inactivation in dogs and humans highlight convergent molecular events that drive cell division in the pathogenesis of osteosarcoma. Cancer Genetics, 276–277, 1–11. https://doi.org/10.1016/j.cancergen.2023.05.001

Selvarajah, G. T., Verheije, M. H., Kik, M., Slob, A., Rottier, P. J. M., Mol, J. A., & Kirpensteijn, J. (2012). Expression of epidermal growth factor receptor in canine osteosarcoma: Association with clinicopathological parameters and prognosis. Veterinary Journal, 193(2), 412–419. https://doi.org/10.1016/j.tvjl.2012.02.009

Shan, Z. Z., Chen, P. N., Wang, F., Wang, J., & Fan, Q. X. (2017). Expression of P-EGFR and P-Akt protein in esophageal squamous cell carcinoma and its prognosis. Oncology Letters, 14(3), 2859–2863. https://doi.org/10.3892/ol.2017.6526

Shang, B., Liu, Y., Jiang, S., & Liu, Y. (2015). Prognostic value of tumor-infiltrating FoxP3+ regulatory T cells in cancers: a systematic review and meta-analysis. Scientific Reports, 5(1), 15179. https://doi.org/10.1038/srep15179

Singh, A. J., & Gray, J. W. (2021). Chemokine signaling in cancer-stroma communications. In Journal of Cell Communication and Signaling (Vol. 15, Issue 3, pp. 361–381). Springer Science and Business Media B.V. https://doi.org/10.1007/s12079-021-00621-7

So, L., & Fruman, D. A. (2012). PI3K signalling in B- and T-lymphocytes: new developments and therapeutic advances. Biochemical Journal, 442(3), 465–481. https://doi.org/10.1042/BJ20112092

Sobral-Leite, M., Salomon, I., Opdam, M., Kruger, D. T., Beelen, K. J., van der Noort, V., van Vlierberghe, R. L. P., Blok, E. J., Giardiello, D., Sanders, J., Van de Vijver, K., Horlings, H. M., Kuppen, P. J. K., Linn, S. C., Schmidt, M. K., & Kok, M. (2019). Cancer-immune interactions in ER-positive breast cancers: PI3K pathway alterations and tumor-infiltrating lymphocytes. Breast Cancer Research, 21(1), 90. https://doi.org/10.1186/s13058-019-1176-2

Stefano, S., & Giovanni, S. (2019). The PTEN tumor suppressor gene in soft tissue sarcoma. In Cancers (Vol. 11, Issue 8). MDPI AG. https://doi.org/10.3390/cancers11081169

Taddei, M. L., Giannoni, E., Comito, G., & Chiarugi, P. (2013). Microenvironment and tumor cell plasticity: An easy way out. Cancer Letters, 341(1), 80–96. https://doi.org/10.1016/j.canlet.2013.01.042

Tewari, D., Patni, P., Bishayee, A., Sah, A. N., & Bishayee, A. (2022). Natural products targeting the PI3K-Akt-mTOR signaling pathway in cancer: A novel therapeutic strategy. In Seminars in Cancer Biology (Vol. 80, pp. 1–17). Academic Press. https://doi.org/10.1016/j.semcancer.2019.12.008

Torrigiani, F., Pierini, A., Lowe, R., Simčič, P., & Lubas, G. (2019). Soft tissue sarcoma in dogs: A treatment review and a novel approach using electrochemotherapy in a case series. Veterinary and Comparative Oncology, 17(3), 234–241. https://doi.org/10.1111/vco.12462

Wang, G., Wu, M., Maloneyhuss, M. A., Wojcik, J., Durham, A. C., Mason, N. J., & Roth, D. B. (2017). Actionable mutations in canine hemangiosarcoma. PLoS ONE, 12(11). https://doi.org/10.1371/journal.pone.0188667

Weng, W. H., Yu, K. J., Li, L. C., Pang, Y. J., Chen, Y. T., Pang, S. T., & Chuang, C. K. (2020). Low PTEN expression and overexpression of phosphorylated AktSer473 and AktThr308 are associated with poor overall survival in upper tract urothelial carcinoma. Oncology Letters, 20(6). https://doi.org/10.3892/OL.2020.12210

Wouters, M. C. A., & Nelson, B. H. (2018). Prognostic Significance of Tumor-Infiltrating B Cells and Plasma Cells in Human Cancer. Clinical Cancer Research, 24(24), 6125–6135. https://doi.org/10.1158/1078-0432.CCR-18-1481

Yasumaru, C. C., Xavier, J. G., Strefezzi, R. D. F., & Salles-Gomes, C. O. M. (2021). Intratumoral T-Lymphocyte Subsets in Canine Oral Melanoma and Their Association With Clinical and Histopathological Parameters. Veterinary Pathology, 58(3), 491–502. https://doi.org/10.1177/0300985821999321

Yu, L., Wei, J., & Liu, P. (2022). Attacking the PI3K/Akt/mTOR signaling pathway for targeted therapeutic treatment in human cancer. In Seminars in Cancer Biology (Vol. 85, pp. 69–94). Academic Press. https://doi.org/10.1016/j.semcancer.2021.06.019

APPENDICES

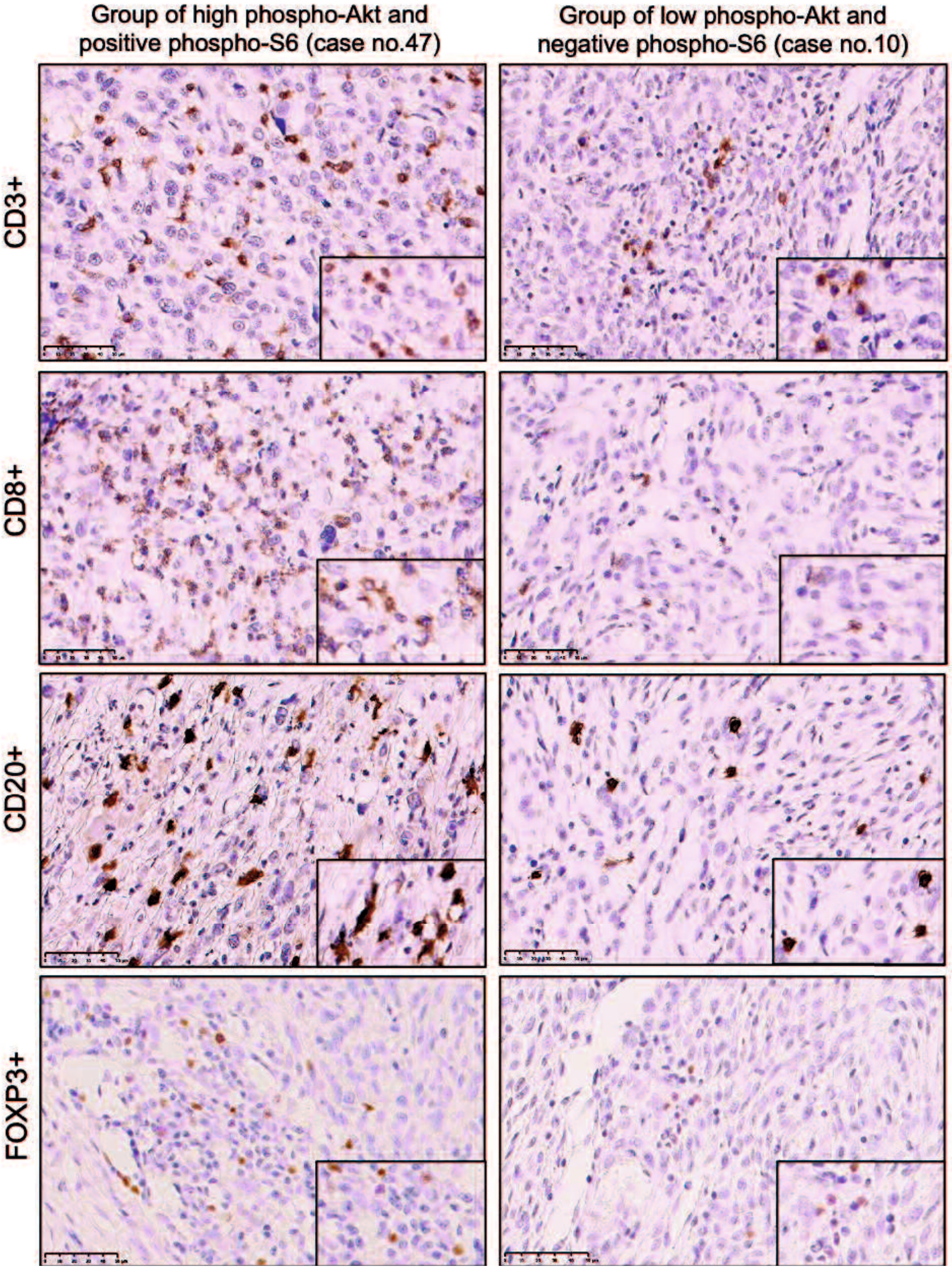

Supplementary Figure I. *Representative Immunolabeling on CD3+ T cells, CD8+ T cells, CD20+ B cells, and FOXP3+ Treg cells. The image on the left column shows the tumor-infiltrating lymphocytes (TILs) density in a sample with high phospho-AKT and positive phospho-S6 staining (case number 47). In contrast, the figure in the right column shows the TILs density in a sample with low phospho-AKT and negative phospho-S6 staining (case number 10) (HPF 400×, scale bar 50 µm).*

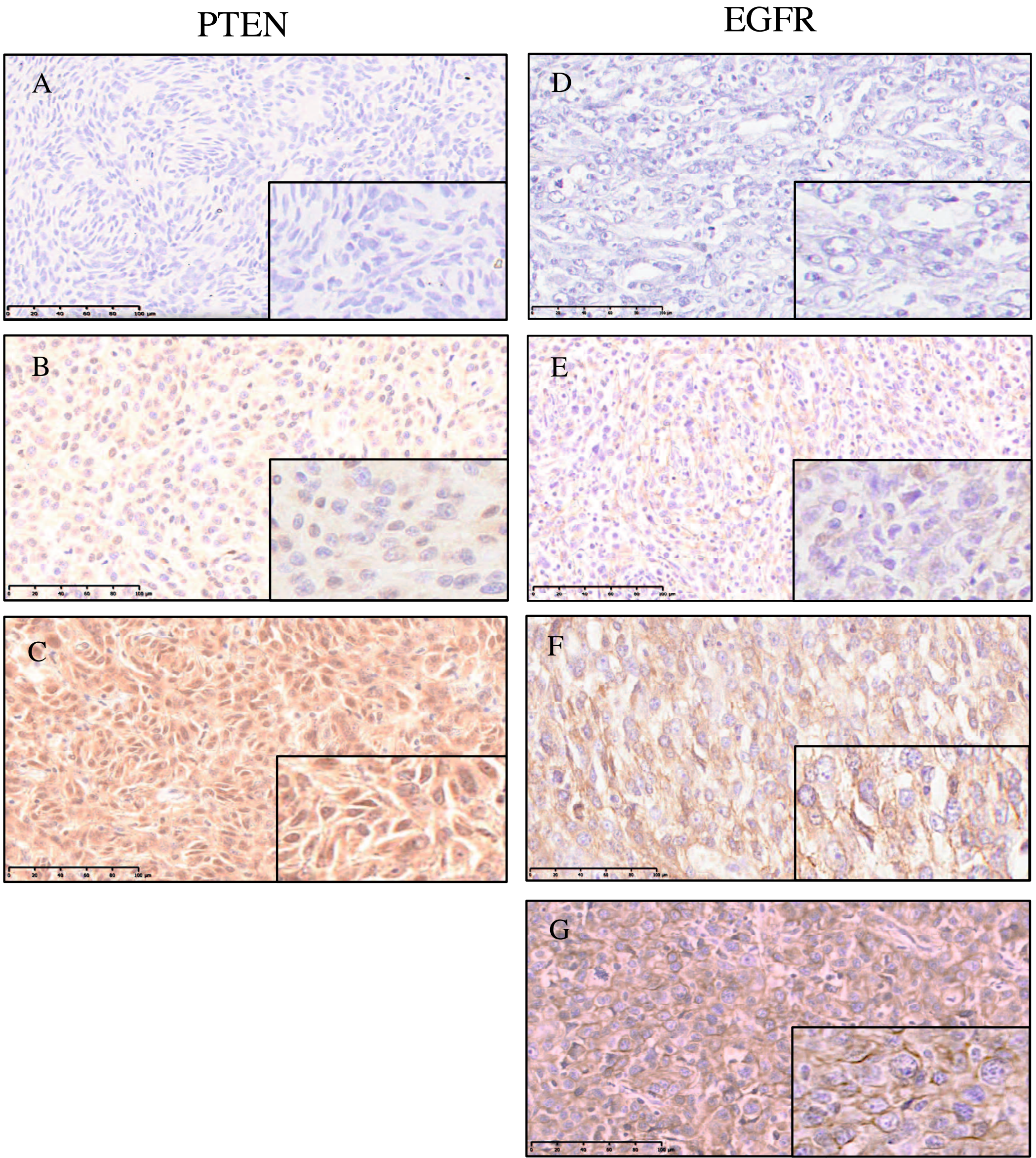

Supplementary Figure II. *Representative immunolabeling score of PTEN and EGFR expression in STS tumor. The figures on the left column show examples of PTEN negative expression (A), weak expression (B), and normal expression (C). The figures on the right column show examples of EGFR negative expression (D), weak expression (E), moderate expression (F), and strong expression (G) (HPF 400×, scale bar 100 µm).*

Supplementary Table I. *The detailed information and TILs profiles of each case*

Case No.	Clinicopathologic					Tumor Grade	History recurrence / metastasis	phospho-AKT (ratio of positive area)	p-S6 expression	Ki-67 index	TILs density (cells/mm²)			
	Breed	Sex	Age	STS type	Location						CD3+	CD8+	CD20+	FOXP3+
1	Shiba	SF	11y4m	FS	scapula	1	metastasis	3.6	positive	48.4	45.7	0.0	4.6	0.0
2	Dorberman	F	9y10m	FS	nose	1	metastasis	0.0	positive	29.2	257.4	28.9	28.9	38.1
3	Mixed breed	F	10y	FS	scapula	1		3.0	positive	46.6	332.0	306.1		0.0
4	Papillon	SF	12y2m	FS	lumbar	1	metastasis	0.0	negative	12.5	103.6	12.2	27.4	0.0
5	Chihuahua	CM	9y5m	FS	spleen	1	metastasis	0.8	positive	0.0		74.6	19.8	0.0
6				FS		1		0.3	positive	14.1	0.0	0.0	0.0	0.0
7				FS		1		0.0	negative	3.5	64.0	10.7	0.0	0.0
8	Mixed breed	SF	14y	FS	hind limb	1		0.1	negative	4.0	228.5	22.8	25.9	4.6
9	Beagle	CM	12y3m	FS	scapula	2		0.0	negative	21.2	86.8	15.2	13.7	12.2
10	Boxer dog	F	10y2m	FS	forearm	2	metastasis	0.5	negative	11.8	156.9	32.0	50.3	7.6
11	Toy poodle	CM	14y9m	FS	mandible	2	recurrence, metastasis	51.9	positive	40.9		469.1		
12				FS		2		6.5	negative	2.0	699.1	498.0	219.3	22.8
13				FS		2		0.0	negative	23.2	0.0	0.0	0.0	0.0
14	Russell terrier	F	7y	FS	maxilla	2	recurrence	6.9	positive	13.2	456.9	357.9		
15	Mixed breed	CM	17y1m	FS	forearm	3	recurrence	2.3	positive	21.5	243.7	56.4	135.5	22.8
16	Mixed breed	M	12y8m	FS	thigh	3		2.0	positive	24.0	48.7	16.8	7.6	0.0
17	Mixed breed	SF	13y6m	FS	precordium	3		6.7	positive	7.7	18.3	13.7	16.8	0.0
18	Labrador retriever		13y11m	FS	precordium	3		49.1	positive	10.2	428.0	383.8	190.4	0.0
19	Westie		5y	FS	neck	3		2.1	positive	29.1	33.5	9.1	22.8	0.0
20	Chihuahua	CM	12y	FS	forearm	3		10.5	positive	7.1	0.0	0.0	0.0	0.0
21	Labrador retriever	F	1y10m	FS	thigh	3	recurrence	0.8	positive	31.4	80.7	18.3	10.7	6.1
22	Shiba	SF	15y1m	FS	scapula	3		0.4	positive	26.0	62.4	6.1	4.6	0.0
23	Mixed breed	SF	14y	FS	thigh	3		4.4	positive	40.9	1382.9	936.6	239.1	30.5
24	Yorkshire terrier	CM	10y1m	MNST	spinal cord	1		13.1	positive	23.0	459.9	105.1	77.7	0.0
25	Welsh corgi	M	10y	MNST	oral cavity	1		11.7		10.2	595.5			
26	Yorkshire terrier	CM	12y4m	MNST	armpit	1		0.0	positive	30.6	7.6	1.5	4.6	0.0
27	Mini. Dachshund	SF	8y5m	MNST	buttocks	1	recurrence	7.1	positive	26.0	223.9	50.3	124.9	12.2
28	Mixed breed	M	14y	MNST	left thight	1		13.1		16.6	201.0	33.5	9.1	0.0
29	Mini. Dachshund	F	12y	MNST	abdomen	1		0.0	positive	13.4	228.5	169.1		
30	Westie	M	11y11m	MNST	perineural	1		11.5	positive	11.4	207.1	71.6	47.2	0.0
31	Golden retriever		7y10m	MNST	hind limb	1	recurrence	1.0	positive	44.1	82.2	13.7	85.3	24.4
32				MNST		1		0.5	positive	6.2	27.4	4.6	0.0	0.0
33				MNST		1		0.0	positive	9.6	6.1	0.0	12.2	0.0

34	Mixed breed	F	11y	MNST	hind limb	2		0.0	negative	7.4	271.1	47.2	57.9	13.7
35	Yorkshire terrier		13y	MNST	elbow	2		0.0	positive	28.4	2100.2	782.8	635.1	16.8
36	Shiba	CM	11y1m	MNST	abdmen	2		0.0	negative	21.9	0.0	0.0	0.0	0.0
37	Mini. Schnauzer	M	13y6m	MNST	elbow	3		2.3	positive	30.1	0.0	0.0	0.0	0.0
38	Border collie	CM	9y7m	UPS	scapula	1	recurrence	3.5	positive	18.8	0.0	0.0	0.0	0.0
39	Boston terrier	SF	13y	UPS	hip joints	2		12.6	positive	13.0	0.0	0.0	0.0	0.0
40	Border collie	F	6y7m	UPS	forearm	2		0.0	positive	5.4	0.0	0.0	0.0	0.0
41	Mixed breed	M	12y1m	UPS	spleen	2	recurrence	5.7	positive	26.1	123.4	36.6	59.4	0.0
42	Golden retriever	SF	5y8m	UPS	buttocks	2		0.0	negative	15.4	0.0	0.0	0.0	0.0
43	Welsh corgi	M	12y6m	UPS	forearm	2		0.2	positive	31.3	1833.7	776.7	574.2	22.8
44	Mixed breed	SF	9y8m	UPS	forearm	2		0.0	positive	2.5	95.9	4.6	50.3	4.6
45	Beagle	CM	10y11m	UPS	pelvic	2		2.6	positive	51.5	236.1	77.7	47.2	0.0
46	Welsh corgi	CM	11y8m	UPS	forearm	3		1.4	positive	20.2	56.4	4.6	28.9	0.0
47	Golden retriever	CM	10y	UPS	elbow	3		10.5	positive	22.5	935.1	744.7	251.3	39.6
48	Welsh corgi	CM	13y7m	UPS	hind limb	3	recurrence	0.0	negative	35.6	0.0	0.0	0.0	0.0
49	Siberian husky	M	14y	UPS	abdmen	3		1.0	positive	49.2	339.6	123.4	9.1	7.6
50	Siberian husky	F	7y11m	PWT	elbow	1		25.8	positive	23.2	338.1	262.0	179.7	4.6
51	French bulldog	M	11y7m	PWT	buttocks	2	recurrence	58.7	positive	0.6	280.2	184.3	65.5	32.0
52	Toy poodle	M	16y5m	PWT	forearm	2	none	0.0	positive	21.7	0.0	0.0	0.0	0.0
53	Shih tzu	CM	13y10m	PWT	buccal	2	none	0.0		12.1	41.1	3.0	0.0	7.6
54	Cavalier spaniel		9y6m	PWT	forearm	3		21.0	positive	20.1	138.6	105.1	32.0	0.0
55	French bulldog	M	9y7m	PWT	hind limb	3		6.4	positive	27.6	855.9	689.9	268.0	25.9
56	Mini. dachsund	M	10y4m	LMS	spleen	2	metastasis	0.0	positive	58.3	501.1	138.6	161.4	91.4
57	Mini. dachsund	SF	9y6m	LMS	buccal	3		7.6	positive	22.3	374.7	13.7	6.1	15.2
58	Mixed breed	M	10y10m	MXS	forearm	3		10.0	positive	30.9	105.1	38.1	7.6	0.0
59	Standard poodle	SF	6y8m	LPS	precordium	3		9.1	positive	17.7	752.4	68.5	163.0	33.5

FS, fibrosarcoma; MNST, malignant nerve sheath tumor; UPS, undifferentiated pleomorphic sarcoma; PWT, perivascular wall tumor; LMS, leiomyosarcoma; MXS, myxosarcoma; LPS, liposarcoma; M, male; CM, castrated male; F, female; spayed female

*Empty columns indicate no available data

Supplementary Table II. *Result of PTEN, EGFR, and PIK3CA analyses*

Case No.	Clinicopathologic			Tumor characteristics			PTEN (n=36)		EGFR (n=36)		Mutation
	Breed	Sex	Age	STS type	Location	Tumor grade	Score intensity and positive rate	Expression	Score intensity and positive rate	Expression	
1	Shiba	SF	11y4m	FS	scapula	1	4	normal			
2	Dorberman	F	9y10m	FS	nose	1	4	normal	1	weak	EGFR exon 18 (non-sense)
3	Mixed breed	F	10y	FS	scapula	1	4	normal	1	weak	
4	Mixed breed	SF	14y	FS	hind limb	1	3	weak	0	negative	
5	Beagle	CM	12y3m	FS	scapula	2	5	normal	0	negative	
6	Boxer dog	F	10y2m	FS	forearm	2	5	normal	1	weak	
7				FS		2	3	weak	0	weak	
8				FS		2	5	normal	0	negative	
9	Mixed breed	CM	17y1m	FS	forearm	3	3	weak	2	moderate	
10	Mixed breed	M	12y8m	FS	thigh	3	3	weak	2	moderate	
11	Mixed breed	SF	13y6m	FS	precordium	3			2	moderate	
12	Labrador retriever		13y11m	FS	precordium	3			3	strong	
13	Westie		5y	FS	neck	3	3	weak	1	weak	
14	Chihuahua	CM	12y	FS	forearm	3			2	moderate	
15	Labrador retriever	F	1y10m	FS	thigh	3	4	normal	1	weak	
16	Shiba	SF	15y1m	FS	scapula	3	5	normal	1	weak	
17	Yorkshire Terrier	CM	10y1m	MNST	spinal cord	1	2	weak			PIK3CA exon 10 (c.554 A>C)
18	Yorkshire Terrier	CM	12y4m	MNST	armpit	1	4	normal	0	negative	
19	Westie	M	11y11m	MNST	perineural	1	2	weak	1	weak	
20	Golden Retriever		7y10m	MNST	hind limb	1	5	normal	1	weak	
21				MNST		1	4	normal	1	weak	PIK3CA exon 21 (non-sense)
22				MNST		1	5	normal			
23	Yorkshire Terrier		13y	MNST	elbow	2	4	normal	1	weak	
24	Mini Schnauzer	M	13y6m	MNST	elbow	3			0	negative	
25	Border Collie	CM	9y7m	UPS	scapula	1	3	weak	2	moderate	
26	Boston Terrier	SF	13y	UPS	hip joints	2	2	weak	3	strong	
27	Border Collie	F	6y7m	UPS	forearm	2	4	normal			
28	Mixed breed	M	12y1m	UPS	spleen	2	3	weak			
29	Mixed breed	SF	9y8m	UPS	forearm	2	4	normal	1	weak	
30	Beagle	CM	10y11m	UPS	pelvic	2	5	normal	2	moderate	
31	Welsh Corgi	CM	11y8m	UPS	forearm	3	4	normal	1	weak	

32	Golden Retriever	CM	10y	UPS	elbow	3			3	strong	
33	Siberian Husky	M	14y	UPS	abdmen	3	5	normal	1	weak	
34	Siberian Husky	F	7y11m	PWT	elbow	1	5	normal	3	strong	
35	French Bulldog	M	11y7m	PWT	buttocks	2	4	normal			EGFR exon 21 (non-sense)
36	Toy Poodle	M	16y5m	PWT	forearm	2	4	normal	0	negative	
37	Shih Tzu	CM	13y10m	PWT	buccal	2	4	normal	2	moderate	
38	Cavalier Spaniel		9y6m	PWT	forearm	3	3	weak	3	strong	
39	French Bulldog	M	9y7m	PWT	hind limb	3	5	normal	2	moderate	
40	Mini. Dachshund	M	10y4m	LMS	spleen	2	5	normal			
41	Mini. Dachshund	SF	9y6m	LMS	buccal	3	2	weak	3	strong	
42	Mixed breed	M	10y10m	MXS	forearm	3			2	moderate	EGFR exon 21 (c. 868 G>A)
43	Standard Poodle	SF	6y8m	LPS	precordium	3			2	moderate	

FS, fibrosarcoma; MNST, malignant nerve sheath tumor; UPS, undifferentiated pleomorphic sarcoma; PWT, perivascular wall tumor; LMS, leiomyosarcoma; MXS, myxosarcoma; LPS, liposarcoma; M, male; CM, castrated male; F, female; spayed female

*Empty columns indicate no available data